© 2017. Published by The Company of Biologists Ltd | Journal of Cell Science (2017) 130, 1094-1109 doi:10.1242/jcs.191858

RESEARCH ARTICLE

The Rap1–cofilin-1 pathway coordinates actin reorganization and MTOC polarization at the B cell immune synapse

Jia C. Wang, Jeff Y.-J. Lee, Sonja Christian, May Dang-Lawson, Caitlin Pritchard, Spencer A. Freeman* and Michael R. Gold‡

ABSTRACT

B cells that bind antigens displayed on antigen-presenting cells (APCs) form an immune synapse, a polarized cellular structure that optimizes the dual functions of the B cell receptor (BCR), signal transduction and antigen internalization. Immune synapse formation involves polarization of the microtubule-organizing center (MTOC) towards the APC. We now show that BCR-induced MTOC polarization requires the Rap1 GTPase (which has two isoforms, Rap1a and Rap1b), an evolutionarily conserved regulator of cell polarity, as well as cofilin-1, an actin-severing protein that is regulated by Rap1. MTOC reorientation towards the antigen contact site correlated strongly with cofilin-1-dependent actin reorganization and cell spreading. We also show that BCR-induced MTOC polarization requires the dynein motor protein as well as IQGAP1, a scaffolding protein that can link the actin and microtubule cytoskeletons. At the periphery of the immune synapse, IQGAP1 associates closely with F-actin structures and with the microtubule plus-end-binding protein CLIP-170 (also known as CLIP1). Moreover, the accumulation of IQGAP1 at the antigen contact site depends on F-actin reorganization that is controlled by Rap1 and cofilin-1. Thus the Rap1–cofilin-1 pathway coordinates actin and microtubule organization at the immune synapse.

KEY WORDS: Microtubule-organizing center, B cell, Immune synapse, Rap1, Cofilin

INTRODUCTION

In vivo, the differentiation of B-lymphocytes into antibody-producing cells is often initiated by antigen-presenting cells (APCs), such as follicular dendritic cells. These APCs capture antigens and display them on their surface in an intact form that is recognized by the B cell receptor (BCR) (Batista and Harwood, 2009; Cyster, 2010; Heesters et al., 2013). For membrane-associated antigens, BCR-induced reorganization of the actin and microtubule cytoskeletons is critical for the two functions of the BCR, signal transduction and antigen internalization (Batista et al., 2010; Song et al., 2013; Yuseff et al., 2013). Initial BCR signaling at the B-cell–APC interface promotes disassembly of the submembrane actin network and uncouples the actin meshwork from the plasma membrane (Freeman et al., 2011; Treanor et al., 2011, 2010). This increases BCR mobility (Freeman et al., 2015; Treanor et al., 2010), allowing antigen-bound BCRs to form microclusters that recruit signaling enzymes (Harwood and Batista, 2011; Tolar et al., 2009; Treanor et al., 2009). Concomitant actin polymerization at the cell periphery allows the B cell to spread across the antigen-bearing surface, encounter more antigens, and form additional BCR microclusters (Fleire et al., 2006; Song et al., 2013). Subsequent contraction of the B cell membrane (Fleire et al., 2006) is accompanied by microtubule-dependent gathering of BCR microclusters into a central supramolecular activation cluster (cSMAC) (Schnyder et al., 2011) that is characteristic of an immune synapse (IS) (Dustin et al., 2010). At the IS, B cells extract BCR-bound antigens from APCs (Batista et al., 2001). These antigens are internalized and delivered to lysosomes and major histocompatibility complex (MHC) II-containing vesicles via actin- and microtubule-dependent processes (Song et al., 2013; Yuseff et al., 2013). Resulting peptide–MHC-II complexes are presented to T cells, which provide additional signals for B cell activation.

Reorientation of the microtubule network coordinates BCR organization and function at the IS. In response to localized BCR signaling, the microtubule-organizing center (MTOC) moves towards the IS (Reversat et al., 2015; Yuseff et al., 2013, 2011) such that microtubules extend along the inner face of the plasma membrane at the contact site (Schnyder et al., 2011). Dynein motor complexes that are recruited to antigen-bound BCRs then propel BCR microclusters along these juxtamembrane microtubules towards the MTOC, to form the cSMAC (Schnyder et al., 2011). Reorientation of the microtubule network also moves lysosomes and MHC II-containing vesicles towards the IS so that extracted antigens can be efficiently delivered to these compartments (Lankar et al., 2002; Vascotto et al., 2007; Yuseff and Lennon-Duménil, 2015; Yuseff et al., 2011). Thus, signaling pathways that couple IS polarity cues to MTOC reorientation are important for APC-mediated B cell activation.

MTOC reorientation towards the lymphocyte IS is coordinated with remodeling of the actin cytoskeleton. In T cells, MTOC polarization is preceded by clearance of F-actin from the center of the IS (Ritter et al., 2015) and is accompanied by accumulation of F-actin at the periphery of the IS (Stinchcombe et al., 2006). Microtubules associate with this peripheral ring of F-actin (Kuhn and Poenie, 2002). Movement of the MTOC towards the IS is driven by dynein motor complexes (Combs et al., 2006; Martín-Cófreces et al., 2008; Quann et al., 2009; Yi et al., 2013). Although the mechanisms that initiate coordinated reorganization of the actin and microtubule networks at the IS are not fully understood, MTOC polarization towards the IS involves evolutionarily conserved polarity proteins including Cdc42, PKCζ, and the Par polarity complex (Bertrand et al., 2010; Huse, 2012; Reversat et al., 2015; Ritter et al., 2013; Stinchcombe et al., 2006; Stowers et al., 1995; Yuseff et al., 2011).

Department of Microbiology & Immunology and the Life Sciences Institute, University of British Columbia, 2350 Health Sciences Mall, Vancouver, British Columbia, Canada V6T 1Z3.
*Present address: Program in Cell Biology, The Hospital for Sick Kids Research Institute, 686 Bay Street, Toronto, Ontario, Canada M5G 0A4.

‡Author for correspondence (mgold@mail.ubc.ca)

M.R.G., 0000-0003-1222-3191

Received 10 May 2016; Accepted 31 January 2017

Journal of Cell Science (2017) 130, 1094-1109 doi:10.1242/jcs.191858

The Rap1 GTPase (which has two isoforms, Rap1a and Rap1b) controls actin dynamics and organization (Freeman et al., 2011) and is important for establishing cell polarity. Bud1p (also known as Rsr1p), the yeast ortholog of Rap1, controls bud site selection and establishes cell polarity by acting upstream of Cdc42 to initiate polarized actin polymerization and promoting reorientation of microtubules towards the bud site (Chant, 1999; Etienne-Manneville, 2004; Kang et al., 2001). Similarly, mammalian Rap1 acts via Cdc42 to establish neuronal polarity (Schwamborn and Püschel, 2004), and via Cdc42 and the Par3–Par6 protein complex to promote directional migration in T cells (Gérard et al., 2007; Shimonaka et al., 2003).

The role of Rap1 in MTOC polarization towards the IS has not been investigated. In B cells, Rap1 is activated by the BCR (McLeod et al., 1998) and the active GTP-bound form of Rap1 accumulates at the contact site with particulate antigens (Lin et al., 2008). BCR-induced Rap1 activation is also required for actin reorganization at the IS (Freeman et al., 2011; Lin et al., 2008). We now show that Rap1 coordinates actin remodeling and MTOC polarization at the B cell IS and that this involves the actin-severing protein cofilin-1 (hereafter referred to as cofilin), which we previously showed is a downstream target of Rap1 (Freeman et al., 2011).

RESULTS

Microtubules and Rap1 are required for cSMAC formation

When B cells bind artificial lipid bilayers with embedded antigens, BCR microclusters form at the periphery of the cell and then move centripetally along microtubules to coalesce into a cSMAC (Schnyder et al., 2011). To extend this finding to B-cell–APC interactions, we performed real-time imaging of the contact site between A20 B-lymphoma cells expressing a hen egg lysozyme (HEL)-specific BCR and APCs expressing a transmembrane form of HEL fused to GFP. In B cells treated with the microtubule-disrupting drug nocodazole, BCR microclusters formed but did not coalesce into a cSMAC, as they did in control cells (Movie 1). Similarly, using primary B cells expressing a transgenic HEL-specific BCR, we found that siRNA-mediated knockdown of the two Rap1 isoforms, Rap1a and Rap1b (see Fig. 1C), prevented BCR microclusters from coalescing into a cSMAC (Movie 2). Because silencing Rap1 impaired cSMAC formation, a process that depends on microtubules, we asked whether Rap1 controls polarization of the MTOC and microtubule network towards the IS.

BCR-induced MTOC polarization depends on Rap1

Antigens that are immobilized onto beads or planar coverslips, embedded in planar lipid bilayers or expressed on the surface of APCs have been used to create a polarized antigen contact site in order to model events that occur at the IS (Fleire et al., 2006; Freeman et al., 2011; Lin et al., 2008; Reversat et al., 2015; Yuseff et al., 2011). In all cases, B cells initially extend their plasma membrane across the antigen-coated surface (Fig. S1A–C). This requires Rap1-dependent reorganization of the actin cytoskeleton (Freeman et al., 2011; Lin et al., 2008).

To assess the role of Rap1 in BCR-induced MTOC reorientation, we initially used anti-Ig-coated beads to establish a well-defined antigen contact site (Reversat et al., 2015; Yuseff et al., 2011). B cells form an F-actin-rich cup around anti-Ig-coated beads (Lin et al., 2008). The MTOC, which was identified by immunofluorescence as the point of microtubule convergence or by staining for the centrosomal protein pericentrin, moved close to this actin-rich cup (Fig. 1A). Real-time imaging showed that the MTOC moved from its initial position to a location close to the antigen contact site (Movies 3 and 4). In some instances the bead also moved along the surface of the cell. We quantified the extent of BCR-induced MTOC polarization by calculating a polarity index (PI) (Yuseff et al., 2011), as described in Fig. S1D. A PI<1 indicates that the MTOC was oriented towards the bead. A PI≤0.75 was used as a definitive measure of MTOC polarization (Fig. S1E). Primary B cells initiated MTOC polarization towards anti-Ig-coated beads within 5 min and by 30 min >95% of the cells had a PI≤0.75 (Fig. 1B); ∼20% would be expected for a random distribution of MTOC localizations (Fig. S1E; Table S1). Similar results were obtained with A20 B-lymphoma cells (see Fig. 1K, vector control cells), which have been used to study BCR-induced cytoskeletal reorganization and MTOC polarization (Freeman et al., 2011; Lin et al., 2008; Reversat et al., 2015; Schnyder et al., 2011; Treanor et al., 2010; Yuseff et al., 2011).

Importantly, siRNA-mediated silencing of Rap1 blocked BCR-induced polarization of the MTOC towards anti-Ig-coated beads in both primary B cells (Fig. 1C–F) and A20 cells (Fig. 1G–I). To test whether BCR-stimulated activation of Rap1 is required for MTOC reorientation, we used B cell lines that overexpress RapGAPII (also known as RAP1GAP2), a GTPase-activating protein that converts Rap1 into its inactive GDP-bound form (Lin et al., 2008). RapGAPII expression abrogated the ability of anti-Ig-coated beads to stimulate Rap1 activation (Fig. S2A) and inhibited MTOC polarization towards anti-Ig-coated beads in the A20 (Fig. 1J,K; Movie 4) and WEHI-231 B cell lines (Fig. S2B,C).

To assess MTOC reorientation towards APCs, we used Cos-7 cells expressing a transmembrane form of an anti-Igκ antibody that binds to the BCR (Freeman et al., 2011). When B cells contacted these APCs, the MTOC moved adjacent to the cell–cell contact site (Fig. 2A). However, MTOC polarization towards the APC (assessed by calculating PIs as in Fig. S1F) was inhibited by silencing Rap1 in primary B cells (Fig. 2A–D) and by expressing RapGAPII in A20 cells (Fig. 2E–G). Thus, both Rap1 expression and activation are important for B cells to reorient their MTOC towards polarized antigen arrays.

Unlike anti-Ig-coated beads, BCR ligands on APCs are mobile. When Rap1 is depleted or its activation is blocked, B cells interacting with antigen-bearing APCs formed microclusters but did not form a cSMAC (Fig. 2A; Movie 1). We previously showed that blocking Rap1 activation reduced the amount of antigen clustering at the B-cell–APC contact site to ∼30% of that in control cells, and reduced BCR-induced phosphotyrosine signaling to a similar degree (Freeman et al., 2011). To investigate the relationship between BCR signaling strength and MTOC polarization, we generated beads with different surface densities of anti-Ig antibodies. Compared to beads coated with the saturating amount of anti-Ig antibodies used in all other experiments, beads that had 44% of the surface density of anti-Ig antibodies induced 35% as much phosphotyrosine signaling at the B-cell–bead contact site (Fig. S2D–F). Importantly, this reduced amount of BCR signaling was sufficient to cause substantial MTOC polarization, with 53% of the cells having a PI≤0.75 (Fig. S2E,F), compared to ∼20% being a random MTOC localization when using 4.5-µm beads (Table S1). In contrast, when Rap1 was depleted (Fig. 2B–D) or its activation blocked (Fig. 2E–G), the percentage of B-cell–APC conjugates with a PI≤0.75 did not exceed the 37.5% expected for a random distribution of MTOC localizations (PIs are calculated differently for APCs and beads; see Fig. S1D–F). Thus, the decreased antigen gathering and BCR signaling that occurs when Rap1 activation is blocked cannot account for the complete inhibition of MTOC polarization. Rap1 must control additional processes that are important for MTOC reorientation.

Journal of Cell Science (2017) 130, 1094-1109 doi:10.1242/jcs.191858

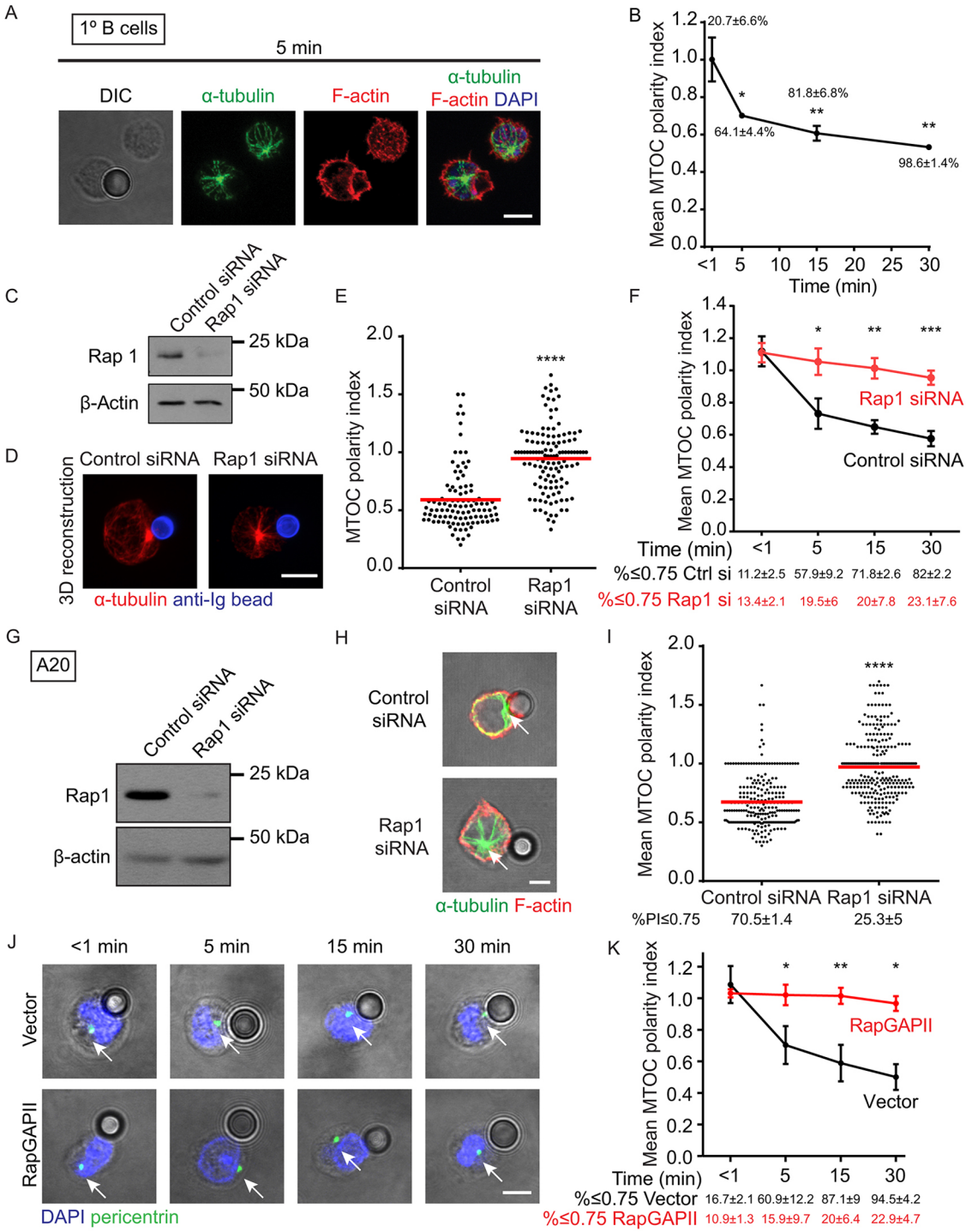

Fig. 1. Rap1 activation is important for MTOC polarization. (A,B) Primary B cells were mixed with 4.5-µm anti-IgM-coated beads for the indicated times and then stained for α-tubulin, F-actin and nuclei (DAPI). Representative *z*-projections (A). In B, MTOC polarity indices (PI) (line graph) were calculated as in Fig. S1D for 14–34 bead–cell conjugates per point. Results are mean±s.e.m. for three experiments. **P*<0.05, ***P*<0.01 compared to the <1 min time point. The percentage of cells with a PI≤0.75 was determined in each experiment and the mean±s.e.m. is shown at each time point (~20% would be random MTOC distribution; see Fig. S1E and Table S1). (C–F) LPS-stimulated primary B cells were transduced with control siRNA or Rap1a and Rap1b siRNAs. Blots show Rap1 knockdown (C). The cells were mixed with 3-µm beads coated with Alexa Fluor 647-conjugated anti-IgM and then stained for α-tubulin. For cells mixed with beads for 30 min, representative 3D reconstruction images are shown (D) along with PIs for >100 conjugates from four experiments (E). *****P*<0.0001. F shows the full timecourse (mean±s.e.m.; four experiments with >16 cells per time point per experiment). **P*<0.05, ***P*<0.01, ****P*<0.001 compared to control siRNA cells at the same time point. For 3-µm beads, having ~11% of cells with a PI≤0.75 would be random MTOC distribution (see Fig. S1E and Table S2). (G–I) A20 cells were transduced with control siRNA or Rap1a and Rap1b siRNAs. Blots show Rap1 knockdown (G). Cells were mixed with 4.5-µm anti-IgG-coated beads for 30 min and stained for α-tubulin and F-actin. Representative confocal *xy* slices overlaid on DIC images (H). PIs and the percentage of cells (mean±s.e.m.) with a PI≤0.75 for >248 conjugates from four experiments (I). *****P*<0.0001. (J,K) Vector control and RapGAPII-expressing A20 cells were mixed with 4.5-µm anti-IgG-coated beads. Pericentrin staining (J). K shows PIs and the percentage of cells with a PI≤0.75 for each time point (mean±s.e.m.; 12–37 conjugates per time point for each of three experiments). **P*<0.05, ***P*<0.01 compared to control cells at the same time point. White arrows indicate the MTOC. Scale bars: 5 µm.

Journal of Cell Science (2017) 130, 1094-1109 doi:10.1242/jcs.191858

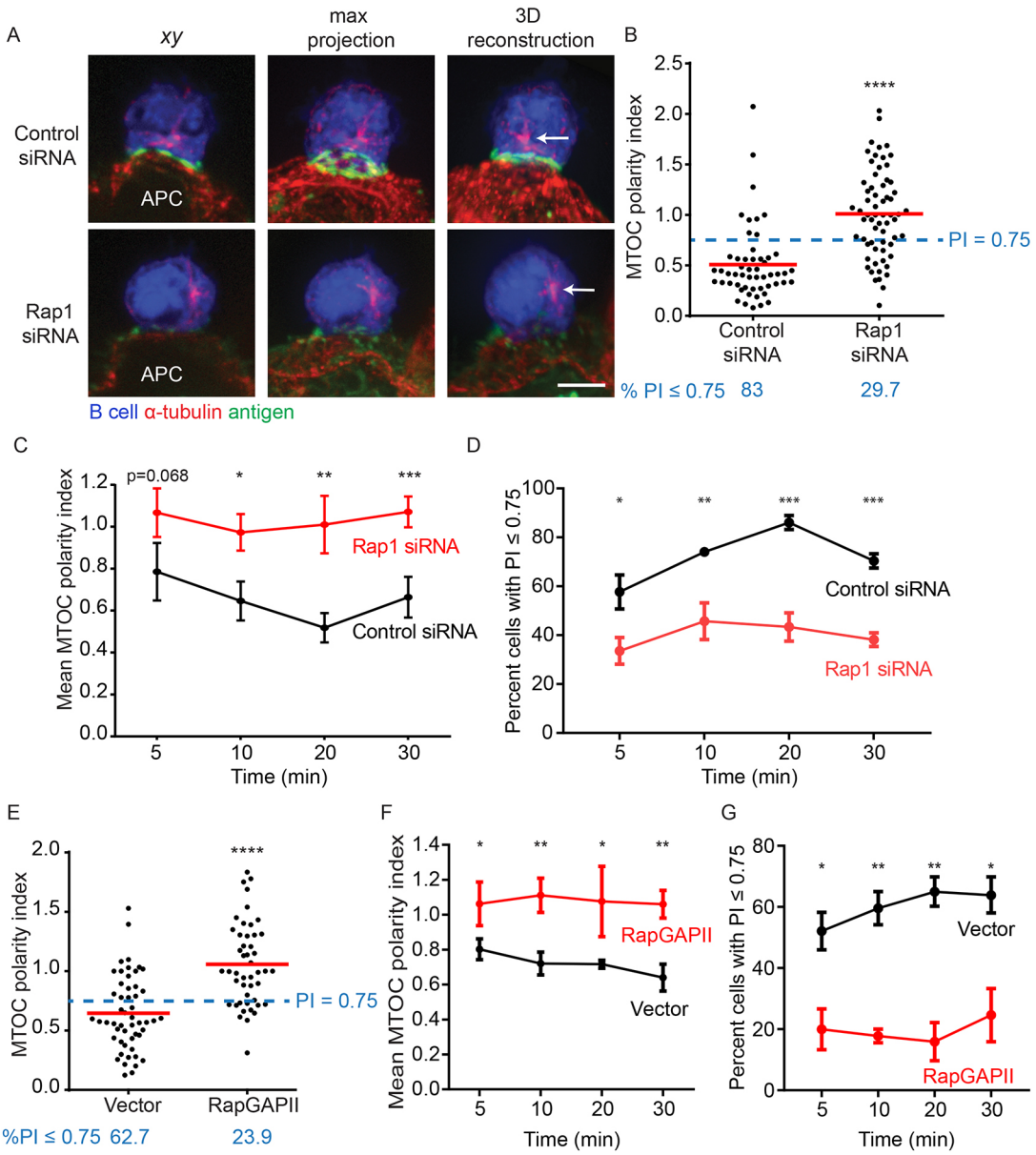

Fig. 2. Rap1 activation is important for MTOC polarization towards APCs. (A–D) LPS-stimulated primary B cells that were transduced with control siRNA or with Rap1a and Rap1b siRNAs were stained with CellTrace Far Red (pseudocolored blue) and mixed with APCs expressing anti-Igκ (antigen). B-cell–APC conjugates were stained for antigen and α-tubulin. Representative images of B cells that were mixed with APCs for 20 min (A). Arrows indicate the MTOC. Scale bar: 5 µm. PIs for >53 B-cell–APC conjugates from four experiments (B; quantified as in Fig. S1F). ****P<0.0001. C and D show the PI values and percentage of cells with a PI≤0.75 for the full timecourse (mean±s.e.m.; four experiments each with >45 conjugates per point). For APC experiments, 37.5% of cells with a PI≤0.75 would be random MTOC distribution. *P<0.05, **P<0.01, ***P<0.001 compared to control siRNA cells at the same time point. (E–G) Vector control and RapGAPII-expressing A20 cells were mixed with anti-Igκ-expressing APCs and then stained for α-tubulin. For A20 cells mixed with APCs for 30 min, PIs were calculated for >47 B-cell–APC conjugates from three experiments (E). ****P<0.0001. F and G shows the full timecourse (mean±s.e.m.; three experiments, each with >35 conjugates per point). *P<0.05, **P<0.01, ***P<0.001 compared to control cells at the same time point.

MTOC polarization requires cofilin-mediated actin severing

The actin and microtubule network are coordinately regulated during processes involving cell polarization (Rodriguez et al., 2003). Indeed, using latrunculin A to depolymerize F-actin abrogated BCR-induced MTOC reorientation (Fig. 3A,B). Thus, an intact actin network is required for MTOC polarization in B cells.

Rap1 promotes actin remodeling at the IS by activating the actin-severing protein cofilin (Freeman et al., 2011). Cofilin-mediated actin severing removes existing actin filaments while creating new barbed ends where the Arp2/3 complex can nucleate branched actin polymerization (Svitkina and Borisy, 1999). When B cells contact antigen-bearing surfaces, both Rap activation and cofilin-mediated actin severing are required for F-actin to be cleared from the center of the contact site and accumulate at the periphery (Freeman et al., 2011). Because BCR-induced MTOC reorientation depends on Rap activation and actin, we asked whether cofilin is involved.

Cofilin is activated by dephosphorylation of serine 3 (S3) (Mizuno, 2013). To assess the role of cofilin-mediated F-actin severing in MTOC polarization, A20 cells were transiently transfected with mCherry-tagged wild-type (WT) cofilin, or with a cofilin mutant that had a phosphomimetic S→D mutation at S3. This S3D mutant, which acts in a dominant-negative manner to

Journal of Cell Science (2017) 130, 1094-1109 doi:10.1242/jcs.191858

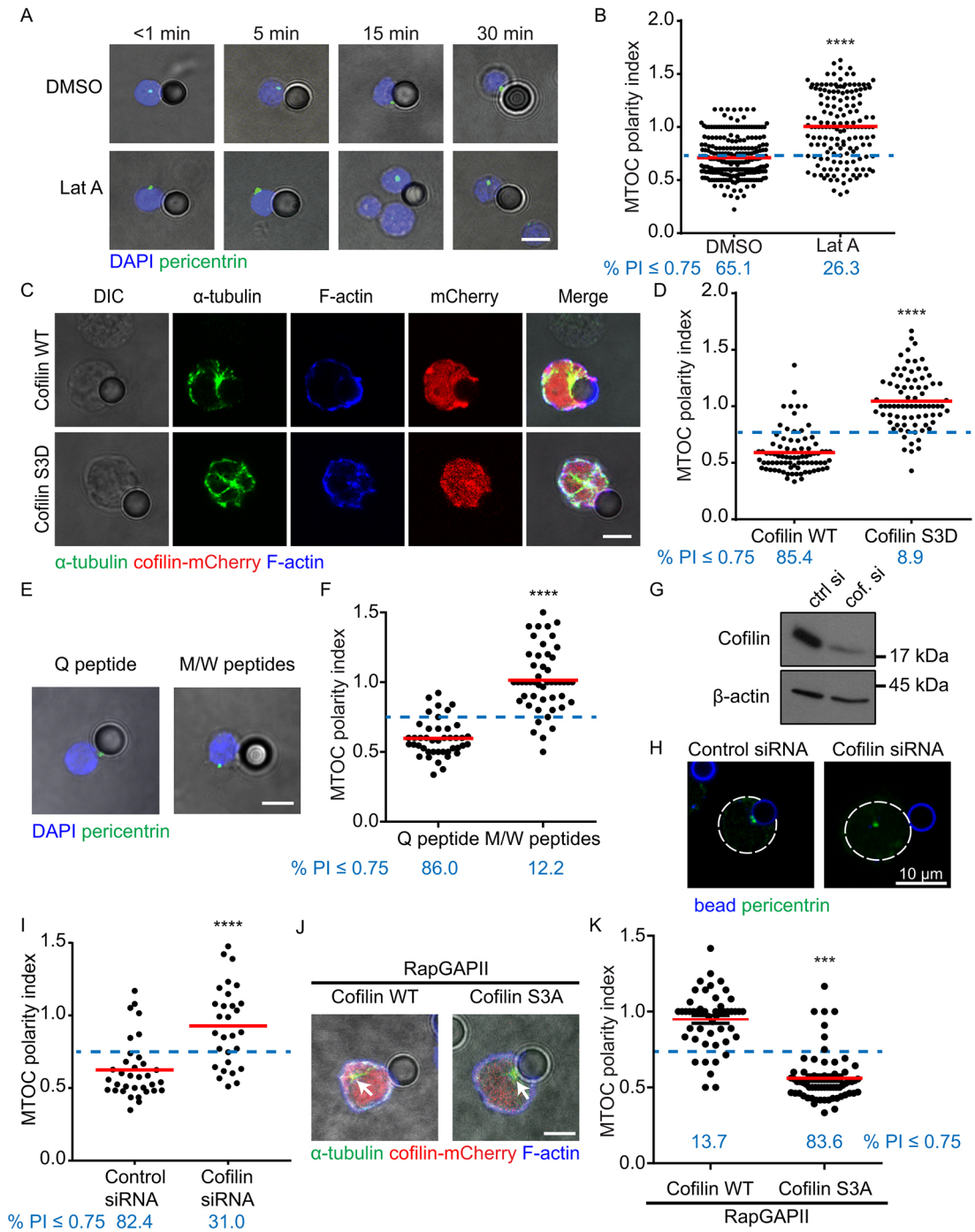

Fig. 3. Cofilin controls BCR-induced MTOC polarization. (A,B) Primary B cells were treated with DMSO or 2 µM latrunculin A (Lat A) for 5 min, mixed with 4.5-µm anti-IgM-coated beads, and then stained for pericentrin. Representative confocal *xy* slices overlaid on DIC images (A). For the 30 min time point, PIs and the percentage of cells with a PI≤0.75 (~20% would be random; see Table S1) were calculated for >156 conjugates from three experiments (B). (C,D) A20 cells expressing either WT or cofilin S3D fused to mCherry were mixed with anti-IgG-coated beads for 30 min. Representative confocal images of α-tubulin and F-actin staining (C). PIs for >79 cells from three experiments (D). (E,F) Primary B cells were treated with the control Q peptide (5 µM) or the M and W cofilin-inhibitory peptides (5 µM each) and then mixed with anti-IgM-coated beads for 30 min. Representative images of pericentrin staining (E). PIs for >43 cells from three experiments (F). (G–I) A20 cells were transduced with control siRNA or cofilin siRNA. Blot shows cofilin knockdown (G). The cells were mixed with anti-IgG-coated beads for 30 min, then stained for pericentrin and for the anti-IgG on the beads. Representative confocal images are shown (H; the dotted line is the outline of the cell) along with PIs for >29 cells. ****P<0.0001. (J,K) RapGAPII-expressing A20 cells transfected with WT cofilin or the constitutively active cofilin S3A fused to mCherry were mixed with anti-IgG-coated beads for 30 min. Representative confocal images of α-tubulin and F-actin staining (J). PIs for >51 cells from three experiments (K). ***P<0.001, ****P<0.0001. Scale bars: 5 µm.

prevent BCR-induced actin reorganization (Freeman et al., 2015, 2011), blocked MTOC polarization towards anti-Ig-coated beads (Fig. 3C,D). Similarly, treating B cells with cell-permeable cofilin-inhibitory peptides (peptides M and W) abrogated MTOC polarization (Fig. 3E,F). These peptides prevent endogenous cofilin from binding to and severing actin filaments (Eibert et al., 2004), and

Journal of Cell Science (2017) 130, 1094-1109 doi:10.1242/jcs.191858

thereby inhibit actin dynamics in B cells (Freeman et al., 2015). MTOC polarization occurred normally in the presence of the control Q peptide in which key residues in the W peptide were changed so as to ablate F-actin binding. Both the cofilin-inhibitory peptides (Eibert et al., 2004) and cofilin S3D (Elam et al., 2015) bind F-actin and prevent severing by endogenous cofilin, raising the possibility that they also block the action of other actin-severing proteins. However, we have previously shown that cofilin is the major actin-severing protein in anti-Ig-stimulated B cells (Freeman et al., 2011), and siRNA-mediated depletion of cofilin also blocked MTOC polarization (Fig. 3G–I). Thus both cofilin and its actin-severing functions are required for BCR-induced MTOC reorientation.

Because Rap1 controls cofilin dephosphorylation and severing activity in B cells (Freeman et al., 2011), we asked whether cofilin acts downstream of Rap1 to promote MTOC polarization. Indeed, expressing the constitutively active cofilin S3A mutant restored BCR-induced MTOC polarization in RapGAPII-expressing A20 cells (Fig. 3J,K). The ability of activated cofilin to bypass a defect in Rap1 activation argues that cofilin is the major downstream effector of Rap1 that couples BCR engagement to MTOC polarization.

At the T cell IS and natural killer (NK) cell IS, the MTOC comes close to the plasma membrane, and this is associated with F-actin clearance at the center of the IS (Rak et al., 2011; Ritter et al., 2015; Stinchcombe et al., 2006). To test whether the MTOC approaches the membrane in response to BCR engagement, and whether this involves cofilin, we employed total internal reflection fluorescence microscopy (TIRFM). This allowed us to visualize only the actin and microtubule structures that were within 100 nm of the interface between a B cell and an anti-Ig-coated coverslip. A20 cells treated with the control Q peptide spread normally and formed a peripheral ring of F-actin surrounding a central region that was depleted of F-actin (Fig. 4A). In these cells, the MTOC and microtubules moved into the 100-nm TIRF plane, with the MTOC in the center of the actin-depleted region (Fig. 4A). When cofilin-mediated F-actin severing was blocked, B cell spreading was impaired, F-actin was not reorganized into a peripheral ring surrounding an actin-poor region, and the ability of the MTOC to approach the plasma membrane at the center of the contact site was significantly reduced (Fig. 4A,B). siRNA-mediated depletion of cofilin also inhibited both actin reorganization and movement of the MTOC into the TIRF plane at 15, 30 and 60 min (Fig. 4C–E; Fig. S3A,B).

To resolve whether Rap1 and cofilin are important for the MTOC to move towards the antigen contact site, versus being retained at that site (i.e. docking), we performed real-time imaging. When A20 cells expressing GFP–α-tubulin and the F-actin probe F-tractin-tdTomato were plated on anti-Ig-coated coverslips, the MTOC moved rapidly towards the coverslip and localized to the center of the region that was cleared of F-actin, with microtubules extending from the MTOC to the peripheral ring of F-actin (Movies 5–7). In contrast, when Rap1 activation was blocked, resulting in impaired cell spreading and actin reorganization, the MTOC did not move close to the antigen contact site (Movie 5). For most RapGAPII-expressing cells, the MTOC did not move at all. In a few, the MTOC shifted slightly towards the antigen contact site but then moved back towards the center of the cell without ever coming close to the antigen contact site. Likewise, when B cells were treated with cofilin-blocking peptides, the cells did not spread, actin reorganization was impaired, and the MTOC did not move towards the antigen contact site (Movies 6 and 7). Kymographs depicting the time evolution of the fluorescence signals in the lowest *xy* plane of the cell also showed that the MTOC moved rapidly into this plane in control cells, but not in cells treated with cofilin-blocking peptides (Fig. 4F). This shows that BCR-induced spreading, actin reorganization, and MTOC polarization are tightly linked and are coordinately regulated by Rap1 and cofilin.

Because BCR-induced spreading on a planar surface correlated with MTOC polarization, we sought to separately assess the roles of BCR signaling and cell spreading. When A20 cells were plated on coverslips coated with anti-Ig antibodies, 75–80% of the cells polarized their MTOC towards the coverslip and had a PI≤0.75 (calculated as in Fig. S1G). In contrast, when the cells were plated on coverslips coated with anti-MHC II antibodies or poly-L-lysine (PLL), the percentage of cells with a PI≤0.75 was similar to the 37.5% value (Fig. S3C,D) expected for a random distribution of MTOC localizations (see Fig. S1). We also assessed the effect of cell spreading in the absence of BCR signaling by plating A20 cells on a pliable fibronectin-coated substrate and using a FlexCell apparatus to apply radial stretch. When stretched, A20 cells flattened, and spread to approximately the same area as cells plated on a rigid anti-Ig-coated substrate (Fig. S3D–F). The stretched cells, which developed abnormal actin structures, did not reorient their MTOC towards the substrate contact site (Fig. S3E,F). The percentage of cells with a PI≤0.75 did not exceed the 37.5% value expected for a random MTOC localization. Hence, spreading is not sufficient to cause MTOC polarization in the absence of BCR signaling. This, however, does not exclude a role for cell spreading in BCR-induced MTOC polarization.

BCR-induced MTOC polarization requires dynein, IQGAP1 and CLIP-170

In T cells, dynein is essential for movement of the MTOC to the IS (Combs et al., 2006; Martín-Cófreces et al., 2008; Quann et al., 2009; Yi et al., 2013). The minus-end-directed movement of dynein along microtubules, which is driven by the ATPase activity of dynein, allows membrane-anchored dynein to reel in the microtubule network and move the MTOC towards the cell membrane. Dynein links BCR microclusters to juxtamembrane microtubules (Schnyder et al., 2011) but it is not known whether dynein activity is required for MTOC polarization. We found that treating A20 cells with either erythro-9-[3-(2-hydroxynonyl)] adenine (EHNA) (Penningroth et al., 1982) or ciliobrevin D (Firestone et al., 2012), both of which inhibit the ATPase activity of dynein, blocked BCR-induced MTOC polarization to the same extent as using nocodazole to depolymerize microtubules (Fig. 5A–D). Although EHNA concentrations 25–200 times greater than we used have profound effects on actin organization (Schliwa et al., 1984), in our experiments F-actin accumulation at the bead contact site occurred normally in B cells treated with these dynein inhibitors (Fig. 5C).

To gain further insights into how actin reorganization promotes MTOC reorientation in B cells, we investigated actin-microtubule crosslinking proteins. IQGAP1 binds F-actin as well as the microtubule plus-end-binding protein CLIP-170 (also known as CLIP1) (Fukata et al., 2002; White et al., 2012). During fibroblast migration, IQGAP1 links microtubules to the actin cortex and coordinates actin reorganization with MTOC reorientation (Fukata et al., 2002; Watanabe et al., 2004; White et al., 2012). We found that depleting either IQGAP1 or CLIP-170 in A20 cells (Fig. 5E,F) blocked MTOC polarization towards anti-Ig-coated beads (Fig. 5G–I) and towards APCs (Fig. 5J,K). Moreover, expressing the C-terminal CLIP-170-binding domain of IQGAP1 (IQGAP1-CT), which can disrupt the interaction between CLIP-170 and endogenous IQGAP1 (Fukata et al., 2002), blocked MTOC polarization towards anti-Ig-coated beads (Fig. S4A,B). Although

Journal of Cell Science (2017) 130, 1094-1109 doi:10.1242/jcs.191858

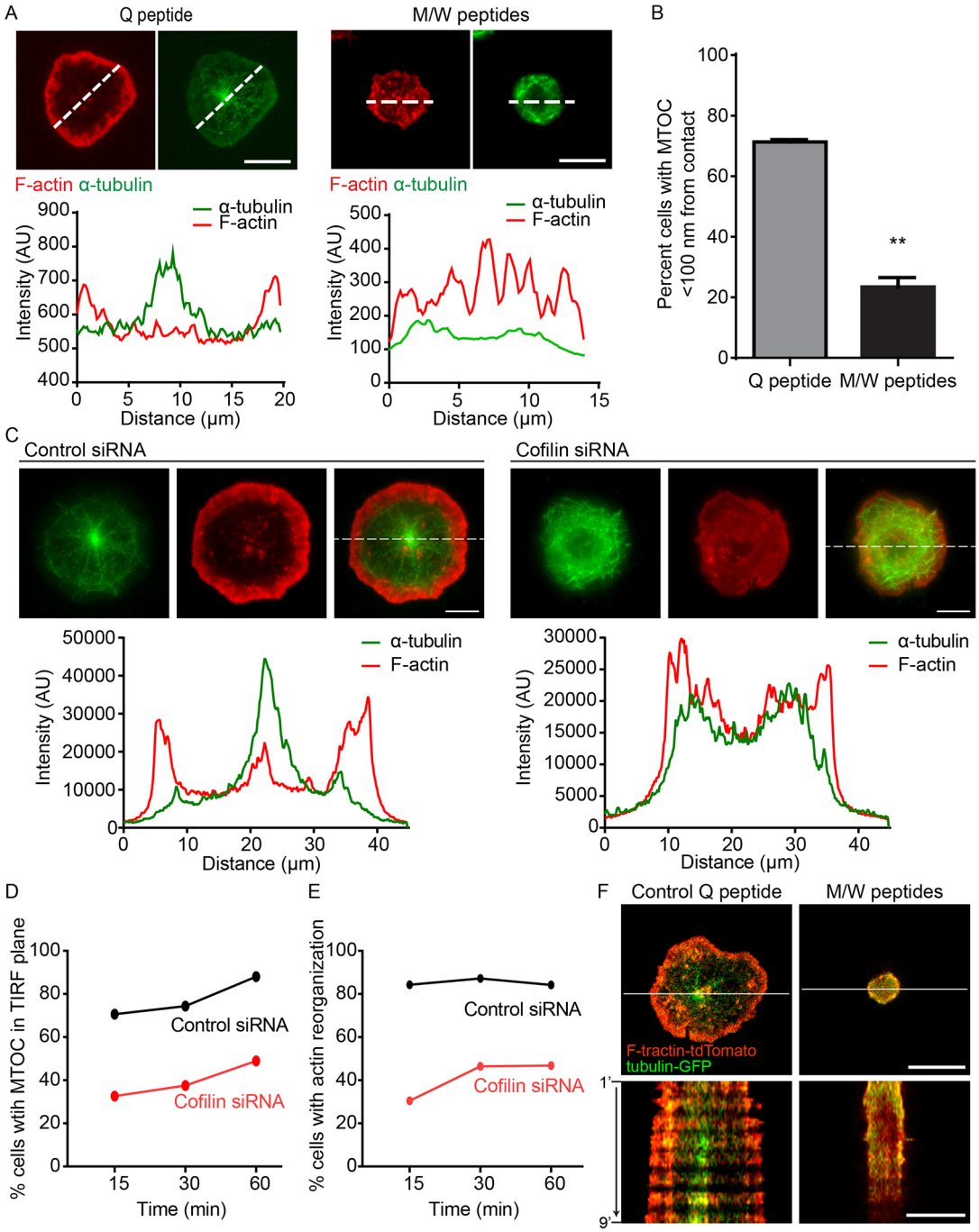

Fig. 4. Cofilin-mediated actin reorganization is required for the MTOC to approach the plasma membrane. (A,B) A20 cells were treated with 5 μM of the control Q peptide (A) or with 5 μM each of the M and W cofilin-blocking peptides and then allowed to spread on anti-IgG-coated coverslips for 15 min. Cells were stained for α-tubulin and F-actin and imaged by TIRFM with a 100-nm depth. Fluorescence intensity profiles along the dotted lines are plotted along with the percentage of cells in which the MTOC was in the TIRF plane (B) (mean±s.e.m.; >41 cells per condition in each of three experiments). $^{**}P<0.01$. (C–E) A20 cells transduced with control siRNA or cofilin siRNA were allowed to spread on anti-IgG-coated coverslips for 15–60 min and imaged by TIRFM with a 100-nm depth. Images of cells at the 15 min time point are shown (C). The percentage of cells with the MTOC within the TIRF plane (D) and the percentage of cells that exhibited a peripheral F-actin ring surrounding a central actin-depleted region (E) are shown for each time point. (F) A20 cells expressing GFP–α-tubulin and F-tractin-tdTomato were treated with control (Q) or cofilin-inhibitory (M and W) peptides, added to anti-Ig-coated coverslips, and imaged in real time for 8 min by confocal microscopy. The kymographs represent a time series of images for the confocal slice closest to the coverslip taken along the white line every 10 s. Scale bars: 10 μm.

this is consistent with the idea that IQGAP1–CLIP-170 interactions are important for BCR-induced MTOC reorientation, IQGAP1-CT could interfere with the ability of CLIP-170 or endogenous IQGAP1 to interact with other proteins. Nevertheless, BCR-induced MTOC polarization clearly requires both IQGAP1 and CLIP-170.

IQGAP1 and CLIP-170 localize to microtubule-actin interfaces

To visualize the relative spatial organization of the actin and microtubule networks, and assess whether the subcellular localizations of IQGAP1 and CLIP-170 could allow them to link

Journal of Cell Science (2017) 130, 1094-1109 doi:10.1242/jcs.191858

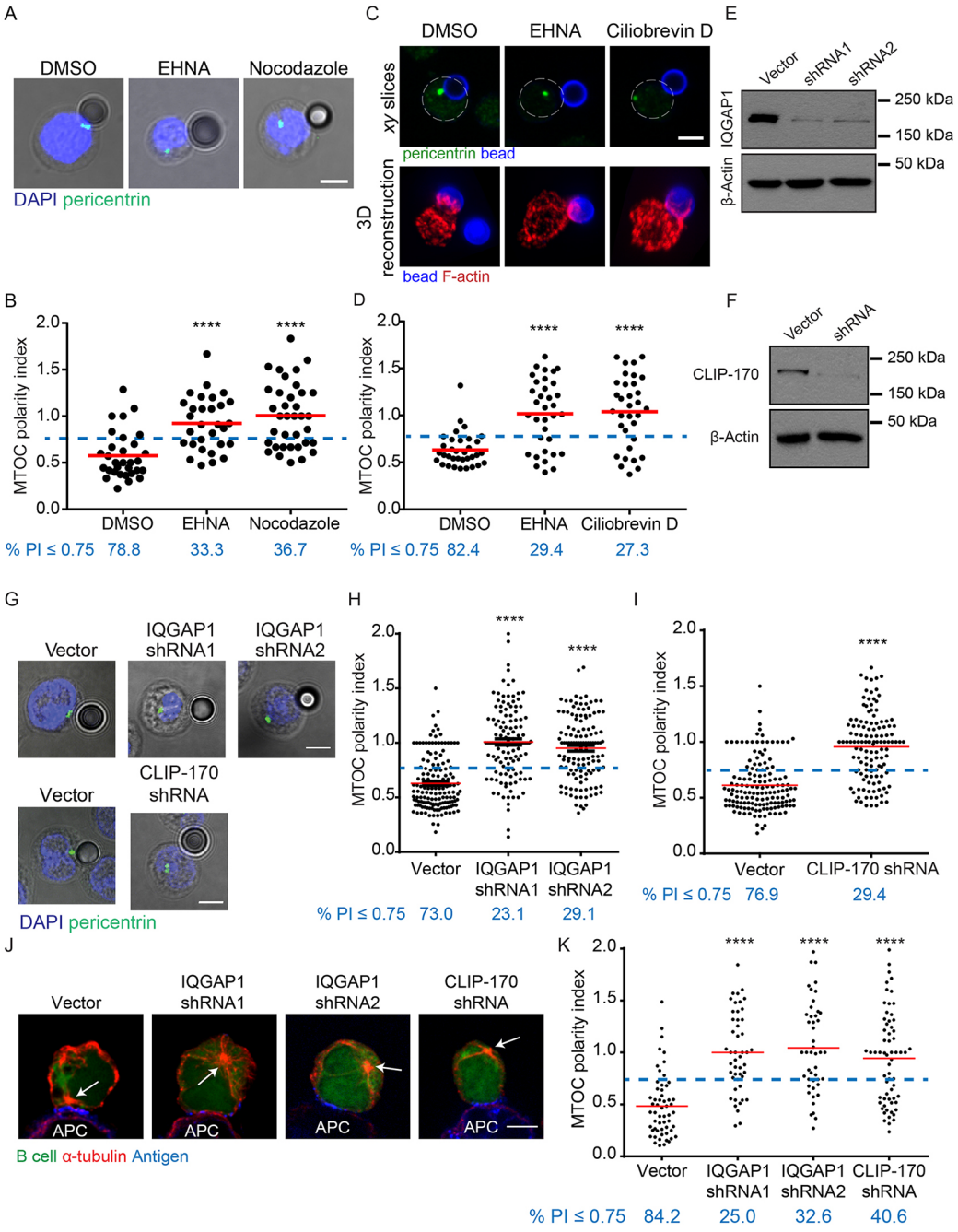

Fig. 5. IQGAP1 and CLIP-170 are required for BCR-induced MTOC reorientation. (A,B) A20 cells were treated with DMSO, 10 µM EHNA or 5 µM nocodazole for 30 min and then mixed with anti-Ig-coated beads for 30 min. Representative confocal images of pericentrin and DAPI staining (A) are shown along with MTOC PIs for >30 cells (B). (C,D) A20 cells were treated with DMSO, 10 µM EHNA or 20 µM ciliobrevin D for 40 min and then mixed for 30 min with beads that had been coated with Alexa Fluor 647-conjugated anti-IgG. Representative *xy* confocal slices of pericentrin-stained cells (C, upper panels; dotted circles indicate the periphery of the cell) are shown along with 3D reconstructions of cells that had been stained for F-actin (C, lower panels). MTOC PIs for >33 cells (D). (E–I) A20 cells were transduced with lentiviruses containing the empty pGipZ vector, IQGAP1 shRNAs or CLIP-170 shRNA. Blots show IQGAP1 (E) and CLIP-170 (F) expression. The cells were mixed with anti-IgG-coated beads for 30 min and stained for pericentrin (G). Graphs show MTOC PIs for control versus IQGAP1 shRNA-expressing cells (H; >127 cells from three experiments) or control versus CLIP-170 shRNA-expressing cells (I; >126 cells from three experiments). The percentage of cells with a PI≤0.75 is indicated (~20% would be random distribution; see Table S1). (J,K) Vector control, IQGAP1 shRNA and CLIP-170 shRNA cells were stained with CMFDA and then mixed with anti-Igκ-expressing APCs for 30 min. *xy* confocal slices of cells stained for α-tubulin and antigen (H). White arrows indicate the MTOC. For each cell population, MTOC PIs were quantified for >81 cells from three experiments (I). The percentage of cells with a PI≤0.75 is indicated (37.5% would be a random distribution). ****P<0.0001. Scale bars: 5 µm.

these two cytoskeletal networks, we plated B cells on anti-Ig-coated coverslips and imaged them by super-resolution stimulated emission depletion (STED) microscopy. As the cells spread radially, F-actin was cleared from the center of the cell while a network of cortical F-actin formed a lamellipodial structure at the cell periphery (Fig. 6A–C). The MTOC was positioned in the center of the area depleted of F-actin (Fig. 6A,B). Microtubules emanating from the MTOC extended along the inner face of the cortical F-actin

Journal of Cell Science

Journal of Cell Science (2017) 130, 1094-1109 doi:10.1242/jcs.191858

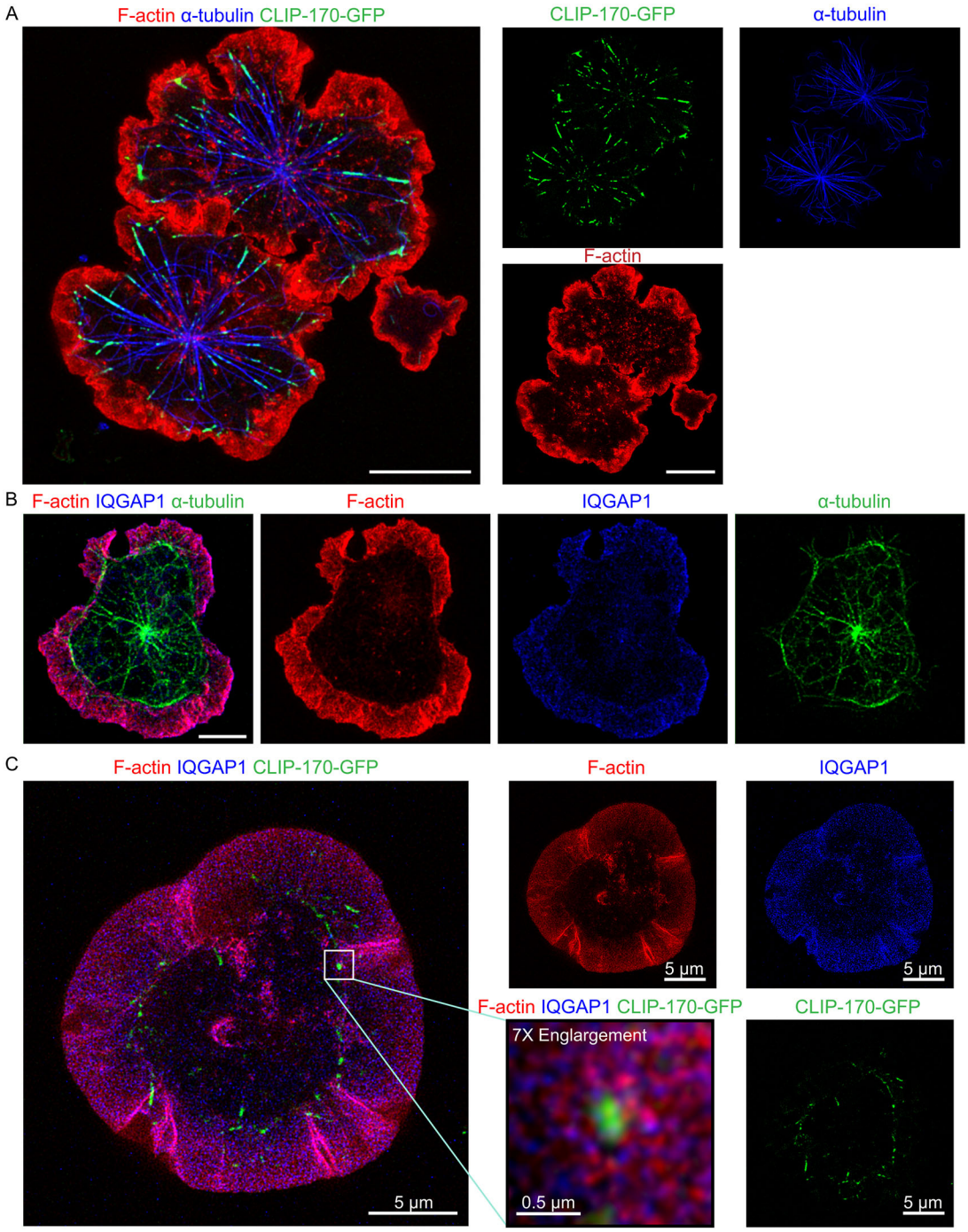

Fig. 6. Colocalization of IQGAP1, CLIP-170, and F-actin. B cells that had been added to anti-IgG-coated coverslips for 15 min were imaged by STED microscopy. (A) A20 cells that had been transfected with CLIP-170–GFP were stained with Rhodamine–phalloidin and with anti-α-tubulin antibody plus an Alexa Fluor 532-conjugated secondary antibody. CLIP-170–GFP fluorescence was imaged directly. An enlarged merged image is shown along with the individual channels. Scale bars: 10 µm. (B) A20 cells were stained with Rhodamine–phalloidin, anti-IQGAP1 antibody plus an Alexa 532-conjugated secondary antibody, and anti-α-tubulin plus an Alexa 488-conjugated secondary antibody. Scale bar: 5 µm. (C) A20 cells expressing CLIP-170–GFP were stained with Rhodamine–phalloidin and with anti-IQGAP1 plus an Alexa Fluor 532-conjugated secondary antibody. CLIP-170–GFP fluorescence was imaged directly. A 7× enlargement of the area in the white box is shown. All images are representative of multiple cells.

ring with some microtubules curling along the interface between the actin cortex and the central actin-depleted region (Fig. 6A,B). Real-time imaging of B cells expressing CLIP-170–GFP, which marks the plus-ends of microtubules, showed that CLIP-170 moved towards the periphery of the cells as they spread on immobilized anti-Ig antibodies (Movies 8 and 9). CLIP-170 extended as far as the cortical ring of F-actin, but not to the edge of the cell (Fig. 6A,C) suggesting that the F-actin ring limits microtubule extension. Indeed, using latrunculin A to deplete F-actin resulted in dramatic microtubule bundling and elongation (Movie 10). This suggests that microtubules interact with the peripheral ring of F-actin and that this regulates microtubule dynamics. STED imaging showed that IQGAP1 was closely associated with the peripheral F-actin network (Fig. 6B) and that the F-actin and IQGAP1 were interwoven with

Journal of Cell Science (2017) 130, 1094-1109 doi:10.1242/jcs.191858

each other at the cell periphery (Fig. 6C). CLIP-170 was embedded in the meshwork of F-actin and IQGAP1 at the inner edge of the peripheral F-actin ring (Fig. 6C), and proximity ligation assays detected multiple sites where IQGAP1 and CLIP-170 were closely associated (Fig. S4C–E). Thus, IQGAP1 and CLIP-170 are in close proximity to each other at the inner face of the peripheral F-actin network, a site where they could link microtubules to the actin cytoskeleton.

Rap1- and cofilin-dependent actin reorganization promotes IQGAP1 accumulation at the periphery of the IS

Because IQGAP1 associates with F-actin at the periphery of the IS (Fig. 6B,C), and Rap1 controls actin organization at the IS (Freeman et al., 2011; Lin et al., 2008), we asked whether Rap1 promotes the accumulation of IQGAP1 at antigen contact sites. Within 5 min of mixing primary B cells with anti-Ig-coated beads (Fig. 7A,B) or anti-Igκ-expressing APCs (see Fig. 7E), both F-actin and IQGAP1 accumulated at the antigen contact site. When F-actin was depleted using latrunculin A, IQGAP1 was not present at the cell cortex and did not accumulate at the contact site (Fig. 7A). This suggests that the localization of IQGAP1 is determined by its interaction with F-actin. Blocking Rap1 activation prevented the accumulation of both F-actin and IQGAP1 at the contact site with anti-Ig-coated beads (Fig. 7B–D). Similarly, Rap1 knockdown prevented IQGAP1 accumulation at B-cell–APC contact sites (Fig. 7E). In both cases, IQGAP1 remained distributed uniformly around the cell cortex (Fig. 7B,E). The effect of Rap1 activation on the localization of IQGAP1 was seen most clearly when B cells were allowed to spread on anti-Ig-coated coverslips. In control A20 cells, IQGAP1 localized to the peripheral F-actin ring and was depleted from the center of the cell where F-actin had been cleared (Fig. 6B,C; Fig. 7F,G). In RapGAPII-expressing A20 cells, which failed to spread, F-actin and IQGAP1 were not cleared from the center of the antigen contact site (Fig. 7F,G). Nevertheless, IQGAP1 still colocalized extensively with F-actin when Rap1 activation was blocked (Fig. 7H,I). Similar results were obtained when cofilin-inhibitory peptides were used to block actin severing (Fig. 8A–C). Although the distribution of F-actin was altered, IQGAP1 remained strongly colocalized with F-actin. Thus, the colocalization of IQGAP1 and F-actin is not dependent on Rap1 or cofilin. Instead, the Rap1–cofilin pathway promotes the accumulation of IQGAP1 at the periphery of antigen contact sites by controlling the organization of the actin network.

These findings suggest that IQGAP1 acts downstream of Rap1 and cofilin to promote MTOC polarization. Consistent with this idea, IQGAP1 knockdown did not inhibit B cell spreading or F-actin reorganization (Fig. S4F,G). Thus, IQGAP1 does not act upstream of or parallel to the Rap1–cofilin pathway to control actin organization in B cells. Additionally, microtubules are not upstream regulators of IQGAP1 localization, as nocodazole did not alter the colocalization of IQGAP1 and F-actin at the periphery of the IS (Fig. 8D–F).

DISCUSSION

The IS is a polarized cell structure similar to the leading edge of a migrating cell or the yeast bud site. Establishing functional patterns of membrane protein organization and vesicular traffic at these sites requires coordinated reorganization of the actin and microtubule cytoskeletons. Rap1 is an evolutionarily conserved regulator of cell polarity that drives actin reorganization at the B cell IS (Lin et al., 2008). We have now shown that Rap1, and its downstream target, the actin-severing protein cofilin, are essential for BCR-induced MTOC polarization towards the IS. Whether Rap1 controls MTOC reorientation in other immune cells is not known. The BCR and TCR both activate Rap1 via phospholipase Cγ-dependent production of diacylglycerol (Katagiri et al., 2004; McLeod et al., 1998), which recruits the Rap1 exchange factor RasGRP2 (also known as CalDAG-GEFI) (Kawasaki et al., 1998) to the plasma membrane. The scaffolding protein ADAP (also known as FYB), which promotes the accumulation or retention of activated Rap1 at the plasma membrane (Kliche et al., 2006), is also required for TCR-induced MTOC polarization (Combs et al., 2006). ADAP is not expressed in B cells (da Silva et al., 1997; Heng et al., 2008). It is not known whether an analogous protein contributes to Rap1 activation and MTOC reorientation in B cells.

This is the first report that cofilin is involved in MTOC polarization towards the IS. We found a strong correlation between BCR-induced MTOC reorientation and the inter-related processes of actin reorganization and cell spreading, which are all dependent on cofilin. In both B and T cells we showed previously that Rap1-dependent activation of cofilin is essential for the formation of a peripheral ring of branched F-actin that drives cell spreading, and for the concomitant depletion of F-actin from the center of the IS (Freeman et al., 2011). This pattern of actin reorganization is also associated with MTOC reorientation to the T cell and NK cell IS (Rak et al., 2011; Ritter et al., 2015; Stinchcombe et al., 2006).

The inhibition of BCR-induced actin reorganization and MTOC polarization caused by depleting Rap1 or blocking its activation was phenocopied by depleting cofilin or inhibiting its function. Moreover, expressing an activated form of cofilin bypassed a block in Rap1 activation and restored BCR-induced spreading, actin reorganization and MTOC polarization. Although other BCR signaling pathways may contribute to BCR-induced MTOC polarization, these results suggest that cofilin is the main Rap1 effector involved in this process.

Antigens on the surface of APCs are mobile, and the spatial organization of antigen-bound BCRs into microclusters is critical for BCR signaling (Harwood and Batista, 2011). Preventing the activation of Rap1 or cofilin reduces the gathering of antigen into BCR microclusters at the B-cell–APC interface, and consequently, reduces BCR signaling (Freeman et al., 2011). Although these functions of the Rap1–cofilin pathway contribute to BCR-induced MTOC polarization, our data suggest that Rap1-dependent processes other than antigen gathering (e.g. actin reorganization and cell spreading) are important for MTOC polarization. Moreover, because movement of the microtubule network close to the antigen contact site promotes cSMAC formation, the reduced antigen gathering and BCR signaling in Rap1-depleted cells could also be secondary to the failure to reorient the MTOC towards the IS.

Linking microtubules to the cortical actin cytoskeleton is essential for controlling microtubule organization and dynamics (Fukata et al., 2002; Rodriguez et al., 2003). IQGAP1 contains both an F-actin-binding domain and a CLIP-170-binding domain (Fukata et al., 2002; White et al., 2012). We found that depleting either IQGAP1 or CLIP-170 prevented BCR-induced MTOC reorientation. This is consistent with a model in which IQGAP1 and CLIP-170 bridge the actin and microtubule cytoskeletons and link BCR-induced actin reorganization to MTOC polarization. However, we cannot rule out other functions of IQGAP1 and CLIP-170, as it has been proposed that CLIP-170 mediates only the initial attachment of microtubules to the cell cortex (Fukata et al., 2002). Other actin-microtubule crosslinking proteins (e.g. spectraplakins; Suozzi et al., 2012), plus-end-binding proteins (e.g. EB1, also

Journal of Cell Science (2017) 130, 1094-1109 doi:10.1242/jcs.191858

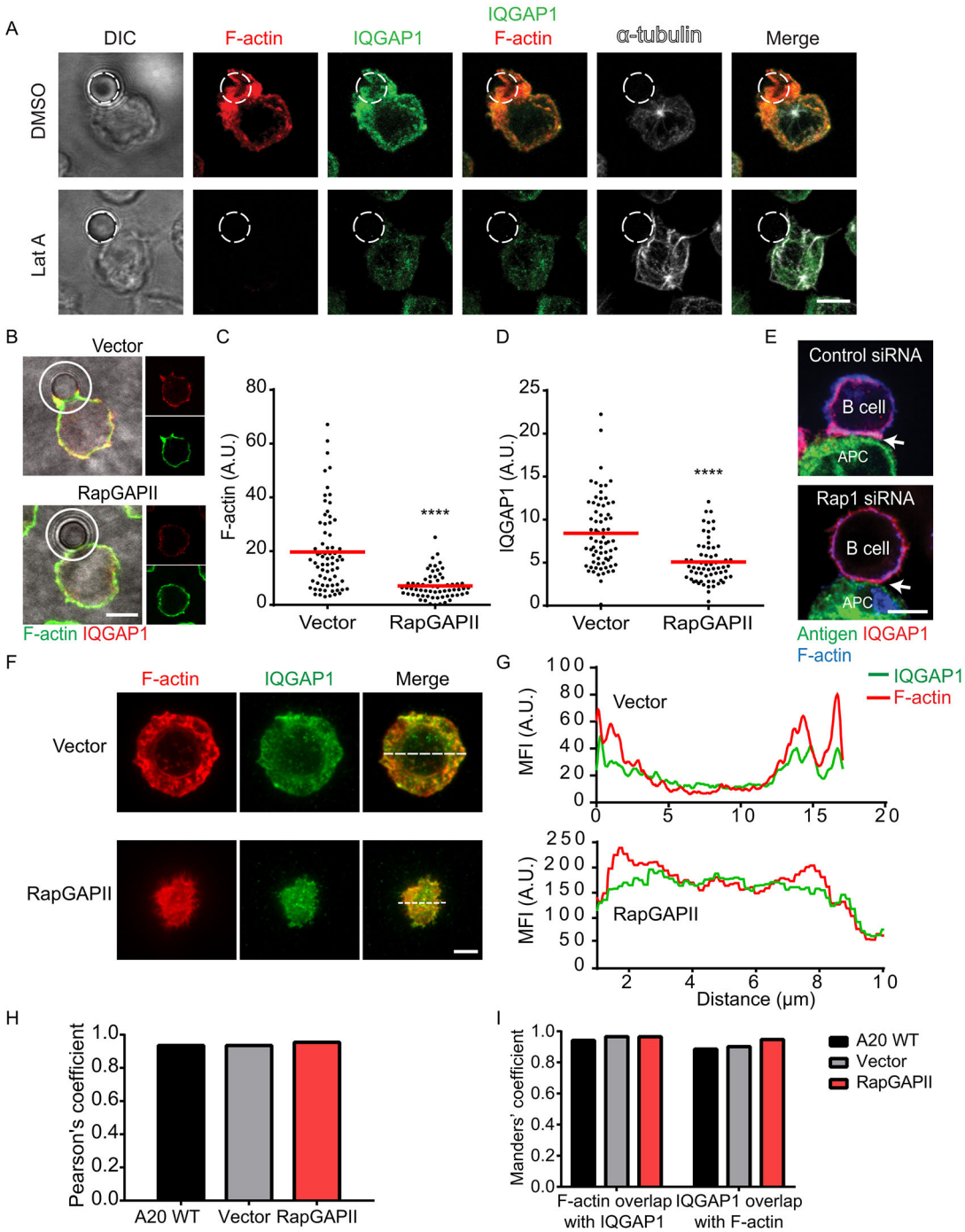

Fig. 7. Rap1 promotes IQGAP1 accumulation at the IS by controlling actin organization. (A) A20 cells were treated with DMSO or 2 µM latrunculin A for 5 min, then mixed with anti-IgG-coated beads for 5 min. Cells were stained for IQGAP1, α-tubulin and F-actin. Confocal *xy* slices of bead–cell conjugates are shown. Dotted circles indicate the bead. (B–D) Vector control and RapGAPII-expressing A20 cells were mixed with anti-IgG-coated beads for 5 min, then stained for IQGAP1 and F-actin. For each conjugate, the corrected fluorescence intensity of F-actin (C) and IQGAP1 (D) within the white circle was quantified (in arbitrary units, AU) for >65 cells from two experiments. (E) LPS-activated primary B cells transfected with control siRNA or with Rap1a and Rap1b siRNAs were mixed with anti-Igκ-expressing APCs for 5 min and then stained for IQGAP1, F-actin and antigen. Arrows show the contact site between the B cell and the APC. (F–I) Vector control and RapGAPII-expressing A20 cells were allowed to spread on anti-IgG-coated coverslips for 15 min, then stained for IQGAP1 and F-actin and imaged by TIRFM or confocal microscopy. TIRFM images (F) and fluorescence profiles along the dotted lines are shown for representative cells (G). Confocal images were used to calculate Pearson's (H) and Manders' (I) coefficients for colocalization of IQGAP1 and F-actin. ****P<0.0001. Scale bars: 5 µm.

known as MAPRE1; Lansbergen and Akhmanova, 2006), or microtubule-capturing proteins (e.g. dynein; Lansbergen and Akhmanova, 2006), may stabilize microtubule attachment to the cell cortex. Interestingly, phosphorylation of CLIP-170 promotes its dissociation from microtubules and this is important for establishing cell polarity in migrating fibroblasts (Nakano et al., 2010). It is not known whether this contributes to BCR-induced MTOC polarization. Nevertheless, our data reveal essential non-redundant roles for IQGAP1 and CLIP-170 in BCR-induced MTOC polarization.

Journal of Cell Science

Journal of Cell Science (2017) 130, 1094-1109 doi:10.1242/jcs.191858

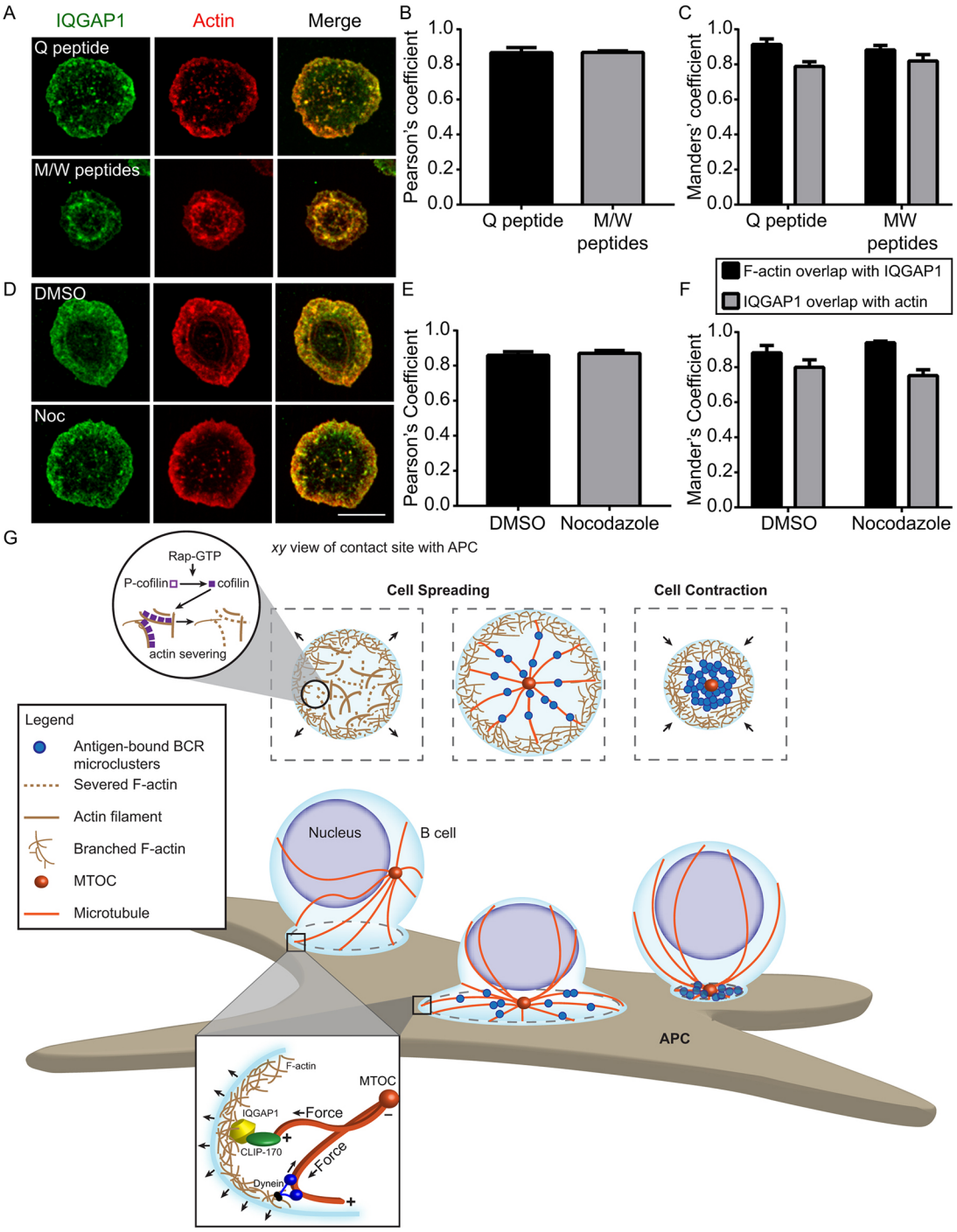

Fig. 8. IQGAP1 colocalization with F-actin and a model for Rap1-dependent MTOC reorientation. (A–F) A20 cells were treated with the control Q peptide or the M and W cofilin-inhibitory peptides (A–C), or with DMSO or 5 µM nocodazole (D–F) before being added to anti-IgG-coated coverslips for 15 min and then stained for IQGAP1 and actin. Representative confocal images are in A and D. Scale bar: 10 µm. Pearson's (B,E) and Manders' (C,F) coefficients for colocalization of IQGAP1 and F-actin are shown in the graphs. (G) Model. APC-bound antigen initiates localized BCR signaling and Rap1 activation. Rap1-GTP promotes cofilin dephosphorylation and stimulates cofilin-mediated actin severing. The resulting clearance of F-actin from the center of the B-cell–APC contact site is coupled to formation of a peripheral ring of branched actin that promotes B cell spreading. IQGAP1, which colocalizes with F-actin at the cell periphery, captures microtubule plus-ends by binding CLIP-170. As the cell spreads, forces are exerted on microtubules that are anchored to the peripheral F-actin ring. This, together with the minus-end-directed movement of cortex-associated dynein along these microtubules, moves the MTOC towards the IS. Dynein motor complexes then move BCR microclusters along juxtamembrane microtubules towards the MTOC to form a cSMAC.

IQGAP1 colocalized with F-actin at the periphery of antigen contact sites, where it was interwoven with actin structures and in close proximity to CLIP-170. Although IQGAP1 can bind to activated Rap1 (Awasthi et al., 2010; Jeong et al., 2007), Rac1 and Cdc42 (Fukata et al., 2002; Watanabe et al., 2004), we found that IQGAP1 localization in B cells was determined primarily by its interaction with F-actin. The activation of Rap1 and cofilin controlled the subcellular localization of both F-actin and IQGAP1

in a coordinated manner. Moreover, IQGAP1 and F-actin colocalized even when Rap1 or cofilin were inhibited. The accumulation of IQGAP1 at adherens junctions is also dependent on F-actin and is ablated by actin-disrupting drugs (Katata et al., 2003). Nevertheless, activated Rac1 and Cdc42 may define specific sites within the actin network to which IQGAP1 is recruited (Fukata et al., 2002).

IQGAP1 may play distinct roles at the IS in different immune cells. IQGAP1 localizes to the NK cell IS and is required for MTOC polarization and the polarization of cytotoxic granules towards target cells (Kanwar and Wilkins, 2011). In contrast, IQGAP1 is dispensable for MTOC polarization in T cells but instead regulates actin organization (Gorman et al., 2012). Depleting IQGAP1 causes excessive F-actin accumulation at the T cell IS and increases cell spreading. In B cells, we found that depleting IQGAP1 blocked MTOC reorientation but did not alter cell spreading or F-actin reorganization at the antigen contact site.

Movement of the MTOC towards the center of the IS is mediated by forces exerted on microtubules. When B cells spread across antigen-bearing surfaces, the outward movement of the peripheral F-actin ring could generate forces that pull on microtubules that are anchored to the cell cortex. This may initiate movement of the MTOC towards the IS. However, simply increasing the substrate contact area by mechanically stretching B cells was not sufficient to move the MTOC to the antigen contact site. Instead, we identified a critical role for dynein in this process, as in T cells (Combs et al., 2006; Martín-Cófreces et al., 2008; Quann et al., 2009; Yi et al., 2013). Dynein can be recruited to the cell cortex (Kuhn and Poenie, 2002; Yi et al., 2013) by binding TCR (Hashimoto-Tane et al., 2011) or BCR microclusters (Schnyder et al., 2011). CLIP-170 also binds dynein and recruits it to the plus-ends of microtubules (Coquelle et al., 2002). Thus, the requirement for CLIP-170 in BCR-induced MTOC polarization could reflect its ability to bind cortical IQGAP1 and recruit dynein. Indeed, NDE1, a protein that binds to both dynein and the CLIP-170-interacting protein LIS1 (also known as PAFAH1B1), is required for dynein to be recruited to the periphery of the T cell IS and for MTOC translocation to the T cell IS (Nath et al., 2016). Whether NDE1- and LIS1-mediated coupling of CLIP-170 to dynein contributes to MTOC polarization in B cells remains to be determined. Dynein can form multiple protein complexes and it is possible that dynein–dynactin complexes, which mediate the coalescence of BCR microclusters into a cSMAC, have distinct functions from the dynein, NDE and LIS1 complexes that have been implicated in MTOC polarization in T cells (Nath et al., 2016).

Our data are consistent with a model (Fig. 8G) in which Rap1- and cofilin-dependent actin reorganization promotes the accumulation of IQGAP1 at the periphery of the IS, thereby determining sites at which IQGAP1 links the actin and microtubule networks, perhaps by binding CLIP-170. This, together with the movement of dynein along microtubules, generates force that moves the MTOC close to the IS. Our findings also support the idea that Rap1 and cofilin are master regulators of cell polarity (Bakal et al., 2007) that are important for establishing polarized cell-cell communication domains.

MATERIALS AND METHODS

Cells

B cells were isolated from spleens of 6- to 12-week-old C57BL/6 or MD4 mice of either sex (Goodnow et al., 1988) (Jackson Laboratories #002595) using a B cell isolation kit (StemCell Technologies). The university animal care committee approved all protocols. The A20 murine IgG^+ B cell line, RAMOS human IgM^+ B cell line and WEHI-231 murine IgM^+ B cell line were from the ATCC. A20 and WEHI-231 cells stably transfected with pMSCVpuro or pMSCVpuro-FLAG-RapGAPII have been described previously (McLeod et al., 2004). A20 cells expressing the HEL-specific D1.3 transgenic BCR (Batista and Neuberger, 1998) were from Facundo Batista (Cancer Research UK, London, UK). B cells were cultured in RPMI-1640 with 10% heat-inactivated fetal calf serum (FCS), 2 mM glutamine, 1 mM pyruvate, 50 µM 2-mercaptoethanol, 50 U/ml penicillin and 50 µg/ml streptomycin (complete medium). Primary B cells were used immediately post isolation or were cultured for 6 h with 5 µg/ml *E. coli* 0111:B4 lipopolysaccharide (LPS; Sigma-Aldrich) before being transfected.

siRNA knockdown

Control siRNA (ON-TARGETplus Non-Targeting Pool, #D-001810-01-05) and siRNA SMARTpools for mouse Rap1a (#L-057058-01-0005), Rap1b (#L-062638-01-0005), and cofilin (#L-058638-01-0005) were from GE Dharmacon. A20 cells or LPS-treated primary B cells (2×10^6) were transduced with 2 µg each of Rap1a siRNA and Rap1b siRNA, or with 2 µg control siRNA, using AMAXA Nucleofector Kit V (Lonza). Cells were cultured 18 h before use. The pro-survival cytokine BAFF (5 ng/ml; R&D Systems) was added to primary B cell cultures.

Lentivirus-mediated expression of shRNAs

pGipZ-based plasmids encoding GFP, puromycin resistance and shRNAs for IQGAP1 (#V3LMM_426631, #V3LMM_426629) or CLIP-170 (#RMM4431-200324779) were from Thermo Scientific. These were co-transfected with pCMV-VSV-G-M5 and pCMV-δR8.91 (from Dorothee von Laer, Medical University of Innsbruck, Austria) into HEK293 T cells (ATCC). Virus particles were collected at 12 h and 36 h post transfection and added to 12-well plates containing A20 cells, which were then centrifuged at 2000 rpm (750 ***g***) for 1 h at 21°C. Cells were cultured 48 h before selection with 4 µg/ml puromycin. GFP-expressing cell populations were enriched by FACS.

Immunoblotting

Cells were lysed in RIPA buffer and analyzed by immunoblotting as described previously (Freeman et al., 2011). Blots were probed with antibodies against Rap1a and Rap1b (Cell Signaling Technologies #4938, 1:1000), cofilin (#sc-8441, 1:1000), IQGAP1 (#sc-10792, 1:1000), CLIP-170 (#sc-25613, 1:3000) or β-actin (#sc-47778, 1:5000) (all Santa Cruz Biotechnology), followed by horseradish peroxidase-conjugated anti-rabbit IgG (Bio-Rad #170-6515, 1:3000) or anti-mouse IgG (Bio-Rad #170-6516, 1:3000) and ECL detection (GE Life Sciences).

Transient transfection

Plasmids encoding WT or mutant forms of cofilin fused to mCherry have been described previously (Freeman et al., 2011). The CLIP-170–GFP construct (Fukata et al., 2002) was from Kozo Kaibuchi (Nagoya University, Nagoya, Japan). LifeAct–mCherry (#54491) and mTagRFP–α-tubulin (#58026) plasmids were from Addgene. F-tractin-tdTomato and -GFP (Yi et al., 2012) were from John Hammer (National Heart, Lung, and Blood Institute, NIH). A20 cells or RAMOS cells (2×10^6) were nucleofected with 2 µg plasmid DNA using AMAXA Nucleofector kit V and used 24 h later.

Inhibitors

Where indicated, cells were treated with nocodazole (Sigma-Aldrich #M1404), EHNA (EMD Millipore #324630), latrunculin A (Enzo Life Sciences #BML-T119) or ciliobrevin D (EMD Millipore #250401). The penetratin-conjugated M (CDYKDDDDKMASGVAVSDGVIK), W (CDYKDDDDKWAPESAPLKSKM) and Q peptides (CDYKDDDDKW-APESAPLQSQM) (Eibert et al., 2004) were synthesized by Biopeptide Inc. (San Diego, CA) (Freeman et al., 2015). B cells (2.5×10^5) were resuspended in 200 µl cold RPMI-1640 with the M and W peptides (5 µM each) or the Q peptide (5 µM). After 1 h on ice, the cells were warmed to 37°C for 5 min before use.

B-cell–APC interactions

Lipofectamine 2000 (Invitrogen) was used to transiently transfect Cos-7 cells (ATCC) with plasmids encoding either a transmembrane form of HEL

fused to GFP (Batista et al., 2001) or a transmembrane form of a single-chain anti-Igκ antibody (Ait-Azzouzene et al., 2005; Freeman et al., 2011). B cells were stained with CellTrace Far Red (Thermo Fisher #C34553, 1:5000). For live-cell imaging, HEL–GFP-expressing Cos-7 cells were plated on fibronectin-coated coverslips for 4 h. The medium was replaced with modified HEPES-buffered saline (mHBS; 25 mM HEPES, pH 7.2, 125 mM NaCl, 5 mM KCl, 1 mM $CaCl_2$, 1 mM Na_2HPO_4, 0.5 mM $MgSO_4$, 1 mg/ml glucose, 2 mM glutamine, 1 mM sodium pyruvate, 50 µM 2-mercaptoethanol, 2% FCS) before adding HEL-specific B cells and imaging B-cell–APC interactions at 37°C by spinning disk confocal microscopy. Alternatively, Cos-7 APCs were detached using enzyme-free dissociation buffer (0.5 mM EDTA, 100 mM NaCl, 1 mM glucose, pH 7.4) and 2×10^5 were mixed in suspension with 4×10^5 B cells in 200 µl mHBS. After various times at 37°C, the cells were pipetted onto coverslips coated with 0.01% PLL, fixed with 4% paraformaldehyde (PFA) for 10 min at room temperature, immunostained and imaged by spinning disk confocal microscopy.

B cell interactions with anti-Ig-coated beads

Polystyrene beads (4.5 µm diameter; Polysciences, Warrington, PA) were coated with goat anti-mouse IgM (Jackson ImmunoResearch, West Grove, PA; #115-005-020) or anti-mouse IgG (Jackson ImmunoResearch #115-005-008) as described (Lin et al., 2008). Amino Beads (3 µm diameter; Polysciences) were activated overnight at 4°C with 8% glutaraldehyde before adding 20 µg Alexa Fluor 647-conjugated goat anti-mouse IgM (Jackson ImmunoResearch #112-545-175) to 5×10^7 beads for 4 h at room temperature. B cells (2×10^5) were resuspended in mHBS and mixed with 10^6 beads at 37°C. The cells were then adhered to PLL-coated coverslips and fixed with 4% PFA for 10 min at room temperature, or with ice-cold methanol for 10 min at −20°C for pericentrin staining. For live-cell imaging at 37°C, cells were added to coverslips coated with 2 µg/ml anti-MHC II antibodies (Millipore, #MABF33) and imaged by spinning disk confocal microscopy, or added to glass-bottom poly-D-lysine-coated #1.0 dishes (MatTek, Ashland, MA) and imaged by confocal microscopy.

B cell spreading on anti-Ig-coated coverslips

Coverslips were coated with 2 µg/cm^2 goat anti-mouse IgG as described previously (Lin et al., 2008) before adding 10^4 B cells in mHBS. After various times at 37°C, the cells were fixed with 4% PFA for 10 min, permeabilized and stained with anti-α-tubulin antibodies plus phalloidin. Alternatively, cells were imaged in real time at 37°C using spinning disk confocal microscopy or TIRFM.

Immunostaining

Cells that had been fixed onto coverslips were permeabilized for 3 min at room temperature with 0.2% Triton X-100 in PBS, and then blocked with 2% BSA in PBS. Antibodies were diluted in PBS with 2% BSA. Primary antibody and secondary antibody incubations were for 40 min at room temperature. F-actin was stained using Rhodamine-, Alexa Fluor 568- or Alexa Fluor 647-conjugated phalloidin (Molecular Probes-Invitrogen, 1:300). Coverslips were mounted onto glass slides using ProLong Gold or Prolong Diamond anti-fade mounting reagent containing DAPI (Molecular Probes, Invitrogen). Primary antibodies were rabbit anti-α-tubulin (Abcam #ab52866, 1:250), rat anti-α-tubulin (Abcam #ab6161, 1:350), rabbit anti-pericentrin (Abcam #ab4448, 1:500), rabbit anti-IQGAP1 (Santa Cruz #sc-10792, 1:250), and mouse anti-GFP (Invitrogen #A11120, 1:400). Goat secondary antibodies (Molecular Probes-Invitrogen, used at 1:250) were Alexa Fluor 488-conjugated anti-rabbit IgG (#A-11034), Alexa Fluor 568-conjugated anti-rabbit IgG (#A-11036), Alexa Fluor 488-conjugated anti-rat IgG (#A-11006), Alexa Fluor 647-conjugated anti-rat IgG (#A-21248), Alexa Fluor 568-conjugated anti-mouse IgG (#A-11031) and Alexa Fluor 647-conjugated anti-mouse IgG (#A-11029).

Microscopy and image analysis

Confocal microscopy was performed using an Olympus IX81/Fluoview FV1000 confocal microscope with a 100× NA 1.40 oil objective. Fluoview v3.0 and v4.0 software (Olympus) were used to analyze images and generate 3D reconstructions. Image analysis and fluorescence quantification were performed using ImageJ. Spinning disk confocal microscopy was performed using a Quorum Technologies system based on a Zeiss Axiovert 200 M microscope with a 100× NA 1.45 oil objective and a QuantEM 512SC Photometrics camera for image acquisition. For fixed cells, *z*-stacks were acquired in 0.3 µm increments. Slidebook v6.0 software (3i Inc., Denver, CO) was used to analyze images and generate 3D reconstructions. TIRF images were acquired at a 100-nm penetration depth using an Olympus cellTIRF 4-line microscopy system consisting of an Olympus IX83 Dual Deck motorized inverted microscope, a 100× NA 1.49 oil objective, and a Photometrics Evolve EM-CCD camera. MetaMorph software (Molecular Devices, Sunnyvale, CA) was used to acquire images. To quantify MTOC polarization, a PI was calculated for each B cell as described in Fig. S1. Distances were determined using Fluoview and ImageJ software. For bead–cell conjugates, a confocal slice through the center of the B cell was used to determine distances. Pearson and Manders coefficients were determined using the ImageJ JACoP plug-in.

Quantification of F-actin and IQGAP1 at bead–cell contact sites

Fluorescence intensities were quantified using ImageJ. An 8.8-µm diameter circular region of interest (ROI) was drawn around the bead at the site of contact with the B cell and the total corrected fluorescence within the ROI was quantified as described (Burgess et al., 2010) using the following equation: Integrated density–[(area of ROI)×(mean background fluorescence per unit area)], where the integrated density is equal to [(area of ROI)×(mean fluorescence per unit area within the ROI)].

STED microscopy

Cells that had spread on anti-Ig-coated coverslips were fixed for 10 min with 3% PFA plus 0.1% glutaraldehyde, then blocked and permeabilized for 10 min at room in blocking buffer (PBS containing 3% BSA and 0.1% Triton X-100). Primary and secondary antibodies (1:100 in blocking buffer) were added sequentially for 30 min at room temperature. Rhodamine–phalloidin (1:100) was added to the secondary antibody solution. Coverslips were mounted onto glass slides using ProLong Diamond anti-fade reagent (Molecular Probes-Invitrogen). Samples were imaged using a Leica TCS SP8 laser scanning STED system equipped with a 592 nm depletion laser, a CX PL APO 100× NA 1.40 oil objective, and a Leica HyD high-sensitivity detector. Image deconvolution was performed using Huygens software (Scientific Volume Imaging, Hilversum, The Netherlands).

Statistical analysis

Two-tailed paired *t*-tests were used to compare mean values for matched sets of samples from multiple experiments. Unpaired *t*-tests were used to compare the means of data pooled from multiple experiments (e.g. dot plots).

Acknowledgements

We thank the UBC Life Sciences Institute Imaging Facility, Linda Matsuuchi, Lisa Osborne and Madison Bolger-Munro for comments on the manuscript, and Kate Choi for technical support.

Competing interests

The authors declare no competing or financial interests.

Author contributions

J.C.W. designed and performed the majority of the experiments, analyzed data and wrote the manuscript; J.Y.-J.L., S.C., M.D.-L. and C.P. performed experiments; S.A.F. performed preliminary experiments and provided feedback; M.R.G. analyzed data and wrote the manuscript.

Funding

This work was supported by the Canadian Institutes of Health Research (MOP-68865 to M.R.G.). J.C.W. was supported by a doctoral scholarship from the Natural Sciences and Engineering Research Council of Canada.

Supplementary information

Supplementary information available online at
http://jcs.biologists.org/lookup/doi/10.1242/jcs.191858.supplemental

References

Ait-Azzouzene, D., Verkoczy, L., Peters, J., Gavin, A., Skog, P., Vela, J. L. and Nemazee, D. (2005). An immunoglobulin C kappa-reactive single chain antibody fusion protein induces tolerance through receptor editing in a normal polyclonal immune system. *J. Exp. Med.* **201**, 817-828.

Awasthi, A., Samarakoon, A., Chu, H., Kamalakannan, R., Quilliam, L. A., Chrzanowska-Wodnicka, M., White, G. C., II and Malarkannan, S. (2010). Rap1b facilitates NK cell functions via IQGAP1-mediated signalosomes. *J. Exp. Med.* **207**, 1923-1938.

Bakal, C., Aach, J., Church, G. and Perrimon, N. (2007). Quantitative morphological signatures define local signaling networks regulating cell morphology. *Science* **316**, 1753-1756.

Batista, F. D. and Harwood, N. E. (2009). The who, how and where of antigen presentation to B cells. *Nat. Rev. Immunol.* **9**, 15-27.

Batista, F. D. and Neuberger, M. S. (1998). Affinity dependence of the B cell response to antigen: a threshold, a ceiling, and the importance of off-rate. *Immunity* **8**, 751-759.

Batista, F. D., Iber, D. and Neuberger, M. S. (2001). B cells acquire antigen from target cells after synapse formation. *Nature* **411**, 489-494.

Batista, F. D., Treanor, B. and Harwood, N. E. (2010). Visualizing a role for the actin cytoskeleton in the regulation of B-cell activation. *Immunol. Rev.* **237**, 191-204.

Bertrand, F., Esquerre, M., Petit, A.-E., Rodrigues, M., Duchez, S., Delon, J. and Valitutti, S. (2010). Activation of the ancestral polarity regulator protein kinase C zeta at the immunological synapse drives polarization of Th cell secretory machinery toward APCs. *J. Immunol.* **185**, 2887-2894.

Burgess, A., Vigneron, S., Brioudes, E., Labbé, J.-C., Lorca, T. and Castro, A. (2010). Loss of human Greatwall results in G2 arrest and multiple mitotic defects due to deregulation of the cyclin B-Cdc2/PP2A balance. *Proc. Natl. Acad. Sci. USA* **107**, 12564-12569.

Chant, J. (1999). Cell polarity in yeast. *Annu. Rev. Cell Dev. Biol.* **15**, 365-391.

Combs, J., Kim, S. J., Tan, S., Ligon, L. A., Holzbaur, E. L. F., Kuhn, J. and Poenie, M. (2006). Recruitment of dynein to the Jurkat immunological synapse. *Proc. Natl. Acad. Sci. USA* **103**, 14883-14888.

Coquelle, F. M., Caspi, M., Cordelieres, F. P., Dompierre, J. P., Dujardin, D. L., Koifman, C., Martin, P., Hoogenraad, C. C., Akhmanova, A., Galjart, N. et al. (2002). LIS1, CLIP-170's key to the dynein/dynactin pathway. *Mol. Cell. Biol.* **22**, 3089-3102.

Cyster, J. G. (2010). B cell follicles and antigen encounters of the third kind. *Nat. Immunol.* **11**, 989-996.

da Silva, A. J., Li, Z., de Vera, C., Canto, E., Findell, P. and Rudd, C. E. (1997). Cloning of a novel T-cell protein FYB that binds FYN and SH2-domain-containing leukocyte protein 76 and modulates interleukin 2 production. *Proc. Natl. Acad. Sci. USA* **94**, 7493-7498.

Dustin, M. L., Chakraborty, A. K. and Shaw, A. S. (2010). Understanding the structure and function of the immunological synapse. *Cold Spring Harb. Perspect. Biol.* **2**, a002311.

Eibert, S. M., Lee, K.-H., Pipkorn, R., Sester, U., Wabnitz, G. H., Giese, T., Meuer, S. C. and Samstag, Y. (2004). Cofilin peptide homologs interfere with immunological synapse formation and T cell activation. *Proc. Natl. Acad. Sci. USA* **101**, 1957-1962.

Elam, W. A., Kang, H., Prochniewicz, E., Nieves-Torres, K., Thomas, D. D. and De La Cruz, E. M. (2015). Phosphomimic S3D cofilin binds actin filaments but does not sever them. *Biophys. J.* **108**, Suppl. 1, 300a.

Etienne-Manneville, S. (2004). Cdc42–the centre of polarity. *J. Cell Sci.* **117**, 1291-1300.

Firestone, A. J., Weinger, J. S., Maldonado, M., Barlan, K., Langston, L. D., O'Donnell, M., Gelfand, V. I., Kapoor, T. M. and Chen, J. K. (2012). Small-molecule inhibitors of the AAA+ ATPase motor cytoplasmic dynein. *Nature* **484**, 125-129.

Fleire, S. J., Goldman, J. P., Carrasco, Y. R., Weber, M., Bray, D. and Batista, F. D. (2006). B cell ligand discrimination through a spreading and contraction response. *Science* **312**, 738-741.

Freeman, S. A., Lei, V., Dang-Lawson, M., Mizuno, K., Roskelley, C. D. and Gold, M. R. (2011). Cofilin-mediated F-actin severing is regulated by the Rap GTPase and controls the cytoskeletal dynamics that drive lymphocyte spreading and BCR microcluster formation. *J. Immunol.* **187**, 5887-5900.

Freeman, S. A., Jaumouillé, V., Choi, K., Hsu, B. E., Wong, H. S., Abraham, L., Graves, M. L., Coombs, D., Roskelley, C. D., Das, R. et al. (2015). Toll-like receptor ligands sensitize B-cell receptor signalling by reducing actin-dependent spatial confinement of the receptor. *Nat. Commun.* **6**, 6168.

Fukata, M., Watanabe, T., Noritake, J., Nakagawa, M., Yamaga, M., Kuroda, S., Matsuura, Y., Iwamatsu, A., Perez, F. and Kaibuchi, K. (2002). Rac1 and Cdc42 capture microtubules through IQGAP1 and CLIP-170. *Cell* **109**, 873-885.

Gérard, A., Mertens, A. E. E., van der Kammen, R. A. and Collard, J. G. (2007). The Par polarity complex regulates Rap1- and chemokine-induced T cell polarization. *J. Cell Biol.* **176**, 863-875.

Goodnow, C. C., Crosbie, J., Adelstein, S., Lavoie, T. B., Smith-Gill, S. J., Brink, R. A., Pritchard-Briscoe, H., Wotherspoon, J. S., Loblay, R. H., Raphael, K. et al. (1988). Altered immunoglobulin expression and functional silencing of self-reactive B lymphocytes in transgenic mice. *Nature* **334**, 676-682.

Gorman, J. A., Babich, A., Dick, C. J., Schoon, R. A., Koenig, A., Gomez, T. S., Burkhardt, J. K. and Billadeau, D. D. (2012). The cytoskeletal adaptor protein IQGAP1 regulates TCR-mediated signaling and filamentous actin dynamics. *J. Immunol.* **188**, 6135-6144.

Harwood, N. E. and Batista, F. D. (2011). The cytoskeleton coordinates the early events of B-cell activation. *Cold Spring Harb. Perspect. Biol.* **3**, a002360.

Hashimoto-Tane, A., Yokosuka, T., Sakata-Sogawa, K., Sakuma, M., Ishihara, C., Tokunaga, M. and Saito, T. (2011). Dynein-driven transport of T cell receptor microclusters regulates immune synapse formation and T cell activation. *Immunity* **34**, 919-931.

Heesters, B. A., Chatterjee, P., Kim, Y.-A., Gonzalez, S. F., Kuligowski, M. P., Kirchhausen, T. and Carroll, M. C. (2013). Endocytosis and recycling of immune complexes by follicular dendritic cells enhances B cell antigen binding and activation. *Immunity* **38**, 1164-1175.

Heng, T. S. and Painter, M. W. and **Immunological Genome Project, Consortium**. (2008). The Immunological Genome Project: networks of gene expression in immune cells. *Nat. Immunol.* **9**, 1091-1094.

Huse, M. (2012). Microtubule-organizing center polarity and the immunological synapse: protein kinase C and beyond. *Front. Immunol.* **3**, 235.

Jeong, H.-W., Li, Z., Brown, M. D. and Sacks, D. B. (2007). IQGAP1 binds Rap1 and modulates its activity. *J. Biol. Chem.* **282**, 20752-20762.

Kang, P. J., Sanson, A., Lee, B. and Park, H. O. (2001). A GDP/GTP exchange factor involved in linking a spatial landmark to cell polarity. *Science* **292**, 1376-1378.

Kanwar, N. and Wilkins, J. A. (2011). IQGAP1 involvement in MTOC and granule polarization in NK-cell cytotoxicity. *Eur. J. Immunol.* **41**, 2763-2773.

Katagiri, K., Shimonaka, M. and Kinashi, T. (2004). Rap1-mediated lymphocyte function-associated antigen-1 activation by the T cell antigen receptor is dependent on phospholipase C-γ1. *J. Biol. Chem.* **279**, 11875-11881.

Katata, T., Irie, K., Fukuhara, A., Kawakatsu, T., Yamada, A., Shimizu, K. and Takai, Y. (2003). Involvement of nectin in the localization of IQGAP1 at the cell-cell adhesion sites through the actin cytoskeleton in Madin-Darby canine kidney cells. *Oncogene* **22**, 2097-2109.

Kawasaki, H., Springett, G. M., Toki, S., Canales, J. J., Harlan, P., Blumenstiel, J. P., Chen, E. J., Bany, I. A., Mochizuki, N., Ashbacher, A. et al. (1998). A Rap guanine nucleotide exchange factor enriched highly in the basal ganglia. *Proc. Natl. Acad. Sci. USA* **95**, 13278-13283.

Kliche, S., Breitling, D., Togni, M., Pusch, R., Heuer, K., Wang, X., Freund, C., Kasirer-Friede, A., Menasche, G., Koretzky, G. A. et al. (2006). The ADAP/SKAP55 signaling module regulates T-cell receptor-mediated integrin activation through plasma membrane targeting of Rap1. *Mol. Cell. Biol.* **26**, 7130-7144.

Kuhn, J. R. and Poenie, M. (2002). Dynamic polarization of the microtubule cytoskeleton during CTL-mediated killing. *Immunity* **16**, 111-121.

Lankar, D., Vincent-Schneider, H., Briken, V., Yokozeki, T., Raposo, G. and Bonnerot, C. (2002). Dynamics of major histocompatibility complex class II compartments during B cell receptor-mediated cell activation. *J. Exp. Med.* **195**, 461-472.

Lansbergen, G. and Akhmanova, A. (2006). Microtubule plus end: a hub of cellular activities. *Traffic* **7**, 499-507.

Lin, K. B., Freeman, S. A., Zabetian, S., Brugger, H., Weber, M., Lei, V., Dang-Lawson, M., Tse, K. W., Santamaria, R., Batista, F. D. et al. (2008). The Rap GTPases regulate B cell morphology, immune-synapse formation, and signaling by particulate B cell receptor ligands. *Immunity* **28**, 75-87.

Martín-Cófreces, N. B., Robles-Valero, J., Cabrero, J. R., Mittelbrunn, M., Gordón-Alonso, M., Sung, C. H., Alarcón, B., Vázquez, J. and Sánchez-Madrid, F. (2008). MTOC translocation modulates IS formation and controls sustained T cell signaling. *J. Cell Biol.* **182**, 951-962.

McLeod, S. J., Ingham, R. J., Bos, J. L., Kurosaki, T. and Gold, M. R. (1998). Activation of the Rap1 GTPase by the B cell antigen receptor. *J. Biol. Chem.* **273**, 29218-29223.

McLeod, S. J., Shum, A. J., Lee, R. L., Takei, F. and Gold, M. R. (2004). The Rap GTPases regulate integrin-mediated adhesion, cell spreading, actin polymerization, and Pyk2 tyrosine phosphorylation in B lymphocytes. *J. Biol. Chem.* **279**, 12009-12019.

Mizuno, K. (2013). Signaling mechanisms and functional roles of cofilin phosphorylation and dephosphorylation. *Cell. Signal.* **25**, 457-469.

Nakano, A., Kato, H., Watanabe, T., Min, K.-D., Yamazaki, S., Asano, Y., Seguchi, O., Higo, S., Shintani, Y., Asanuma, H. et al. (2010). AMPK controls the speed of microtubule polymerization and directional cell migration through CLIP-170 phosphorylation. *Nat. Cell Biol.* **12**, 583-590.

Nath, S., Christian, L., Youngsun Tan, S., Ki, S., Ehrlich, L. I. R. and Poenie, M. (2016). Dynein separately partners with NDE1 and dynactin to orchestrate T cell focused secretion. *J. Immunol.* **197**, 2090-2101.

Penningroth, S. M., Cheung, A., Bouchard, P., Gagnon, C. and Bardin, C. W. (1982). Dynein ATPase is inhibited selectively in vitro by erythro-9-[3-2-(hydroxynonyl)]adenine. *Biochem. Biophys. Res. Commun.* **104**, 234-240.

Journal of Cell Science

Quann, E. J., Merino, E., Furuta, T. and Huse, M. (2009). Localized diacylglycerol drives the polarization of the microtubule-organizing center in T cells. *Nat. Immunol.* **10**, 627-635.
Rak, G. D., Mace, E. M., Banerjee, P. P., Svitkina, T. and Orange, J. S. (2011). Natural killer cell lytic granule secretion occurs through a pervasive actin network at the immune synapse. *PLoS Biol.* **9**, e1001151.
Reversat, A., Yuseff, M.-I., Lankar, D., Malbec, O., Obino, D., Maurin, M., Penmatcha, N. V. G., Amoroso, A., Sengmanivong, L., Gundersen, G. G. et al. (2015). Polarity protein Par3 controls B-cell receptor dynamics and antigen extraction at the immune synapse. *Mol. Biol. Cell* **26**, 1273-1285.
Ritter, A. T., Angus, K. L. and Griffiths, G. M. (2013). The role of the cytoskeleton at the immunological synapse. *Immunol. Rev.* **256**, 107-117.
Ritter, A. T., Asano, Y., Stinchcombe, J. C., Dieckmann, N. M. G., Chen, B.-C., Gawden-Bone, C., van Engelenburg, S., Legant, W., Gao, L., Davidson, M. W. et al. (2015). Actin depletion initiates events leading to granule secretion at the immunological synapse. *Immunity* **42**, 864-876.
Rodriguez, O. C., Schaefer, A. W., Mandato, C. A., Forscher, P., Bement, W. M. and Waterman-Storer, C. M. (2003). Conserved microtubule-actin interactions in cell movement and morphogenesis. *Nat. Cell Biol.* **5**, 599-609.
Schliwa, M., Ezzell, R. M. and Euteneuer, U. (1984). ertytrho-9-[3-(2-Hydroxynonyl)]adenine is an effective inhibitor of cell motility and actin assembly. *Proc. Natl. Acad. Sci. USA* **81**, 6044-6048.
Schnyder, T., Castello, A., Feest, C., Harwood, N. E., Oellerich, T., Urlaub, H., Engelke, M., Wienands, J., Bruckbauer, A. and Batista, F. D. (2011). B cell receptor-mediated antigen gathering requires ubiquitin ligase Cbl and adaptors Grb2 and Dok-3 to recruit dynein to the signaling microcluster. *Immunity* **34**, 905-918.
Schwamborn, J. C. and Püschel, A. W. (2004). The sequential activity of the GTPases Rap1B and Cdc42 determines neuronal polarity. *Nat. Neurosci.* **7**, 923-929.
Shimonaka, M., Katagiri, K., Nakayama, T., Fujita, N., Tsuruo, T., Yoshie, O. and Kinashi, T. (2003). Rap1 translates chemokine signals to integrin activation, cell polarization, and motility across vascular endothelium under flow. *J. Cell Biol.* **161**, 417-427.
Song, W., Liu, C. and Upadhyaya, A. (2013). The pivotal position of the actin cytoskeleton in the initiation and regulation of B cell receptor activation. *Biochim. Biophys. Acta* **1838**, 569-578.
Stinchcombe, J. C., Majorovits, E., Bossi, G., Fuller, S. and Griffiths, G. M. (2006). Centrosome polarization delivers secretory granules to the immunological synapse. *Nature* **443**, 462-465.
Stowers, L., Yelon, D., Berg, L. J. and Chant, J. (1995). Regulation of the polarization of T cells toward antigen-presenting cells by Ras-related GTPase CDC42. *Proc. Natl. Acad. Sci. USA* **92**, 5027-5031.
Suozzi, K. C., Wu, X. and Fuchs, E. (2012). Spectraplakins: master orchestrators of cytoskeletal dynamics. *J. Cell Biol.* **197**, 465-475.
Svitkina, T. M. and Borisy, G. G. (1999). Arp2/3 complex and actin depolymerizing factor/cofilin in dendritic organization and treadmilling of actin filament array in lamellipodia. *J. Cell Biol.* **145**, 1009-1026.
Tolar, P., Sohn, H. W., Liu, W. and Pierce, S. K. (2009). The molecular assembly and organization of signaling active B-cell receptor oligomers. *Immunol. Rev.* **232**, 34-41.
Treanor, B., Harwood, N. E. and Batista, F. D. (2009). Microsignalosomes: spatially resolved receptor signalling. *Biochem. Soc. Trans.* **37**, 1014-1018.
Treanor, B., Depoil, D., Gonzalez-Granja, A., Barral, P., Weber, M., Dushek, O., Bruckbauer, A. and Batista, F. D. (2010). The membrane skeleton controls diffusion dynamics and signaling through the B cell receptor. *Immunity* **32**, 187-199.
Treanor, B., Depoil, D., Bruckbauer, A. and Batista, F. D. (2011). Dynamic cortical actin remodeling by ERM proteins controls BCR microcluster organization and integrity. *J. Exp. Med.* **208**, 1055-1068.
Vascotto, F., Le Roux, D., Lankar, D., Faure-André, G., Vargas, P., Guermonprez, P. and Lennon-Dumenil, A.-M. (2007). Antigen presentation by B lymphocytes: how receptor signaling directs membrane trafficking. *Curr. Opin. Immunol.* **19**, 93-98.
Watanabe, T., Wang, S., Noritake, J., Sato, K., Fukata, M., Takefuji, M., Nakagawa, M., Izumi, N., Akiyama, T. and Kaibuchi, K. (2004). Interaction with IQGAP1 links APC to Rac1, Cdc42, and actin filaments during cell polarization and migration. *Dev. Cell* **7**, 871-883.
White, C. D., Erdemir, H. H. and Sacks, D. B. (2012). IQGAP1 and its binding proteins control diverse biological functions. *Cell. Signal.* **24**, 826-834.
Yi, J., Wu, X. S., Crites, T. and Hammer, J. A., III (2012). Actin retrograde flow and actomyosin II arc contraction drive receptor cluster dynamics at the immunological synapse in Jurkat T cells. *Mol. Biol. Cell* **23**, 834-852.
Yi, J., Wu, X., Chung, A. H., Chen, J. K., Kapoor, T. M. and Hammer, J. A. (2013). Centrosome repositioning in T cells is biphasic and driven by microtubule end-on capture-shrinkage. *J. Cell Biol.* **202**, 779-792.
Yuseff, M. I. and Lennon-Duménil, A. M. (2015). B cells use conserved polarity cues to regulate their antigen processing and presentation functions. *Front. Immunol.* **6**, 251.
Yuseff, M.-I., Reversat, A., Lankar, D., Diaz, J., Fanget, I., Pierobon, P., Randrian, V., Larochette, N., Vascotto, F., Desdouets, C. et al. (2011). Polarized secretion of lysosomes at the B cell synapse couples antigen extraction to processing and presentation. *Immunity* **35**, 361-374.
Yuseff, M.-I., Pierobon, P., Reversat, A. and Lennon-Duménil, A. M. (2013). How B cells capture, process and present antigens: a crucial role for cell polarity. *Nat. Rev. Immunol.* **13**, 475-486.